Published online: March 31, 2015

Article

SOURCE DATA | TRANSPARENT PROCESS | OPEN ACCESS

THE EMBO JOURNAL

Insm1 cooperates with Neurod1 and Foxa2 to maintain mature pancreatic β-cell function

Shiqi Jia[1,**,‡], Andranik Ivanov[2,‡], Dinko Blasevic[1], Thomas Müller[1], Bettina Purfürst[3], Wei Sun[4,†], Wei Chen[4], Matthew N Poy[5], Nikolaus Rajewsky[2] & Carmen Birchmeier[1,*]

Abstract

Key transcription factors control the gene expression program in mature pancreatic β-cells, but their integration into regulatory networks is little understood. Here, we show that Insm1, Neurod1 and Foxa2 directly interact and together bind regulatory sequences in the genome of mature pancreatic β-cells. We used *Insm1* ablation in mature β-cells in mice and found pronounced deficits in insulin secretion and gene expression. Insm1-dependent genes identified previously in developing β-cells markedly differ from the ones identified in the adult. In particular, adult mutant β-cells resemble immature β-cells of newborn mice in gene expression and functional properties. We defined Insm1, Neurod1 and Foxa2 binding sites associated with genes deregulated in *Insm1* mutant β-cells. Remarkably, combinatorial binding of Insm1, Neurod1 and Foxa2 but not binding of Insm1 alone explained a significant fraction of gene expression changes. Human genomic sequences corresponding to the murine sites occupied by Insm1/Neurod1/Foxa2 were enriched in single nucleotide polymorphisms associated with glycolytic traits. Thus, our data explain part of the mechanisms by which β-cells maintain maturity: Combinatorial Insm1/Neurod1/Foxa2 binding identifies regulatory sequences that maintain the mature gene expression program in β-cells, and disruption of this network results in functional failure.

Keywords development; differentiation; Insm1; maturation; metabolisms; pancreatic beta cells

Subject Categories Chromatin, Epigenetics, Genomics & Functional Genomics; Development & Differentiation; Molecular Biology of Disease

DOI 10.15252/embj.201490819 | Received 16 December 2014 | Revised 26 February 2015 | Accepted 10 March 2015 | Published online 31 March 2015

The EMBO Journal (2015) 34: 1417–1433

Introduction

During terminal differentiation of cells, gene expression programs are established that are then faithfully maintained throughout the lifetime of mature cells (Holmberg & Perlmann, 2012). The ontogeny of pancreatic β-cells, the insulin-secreting cells of the body, has been studied extensively, and a hierarchically controlled transcription factor network that determines β-cell specification and differentiation has been defined. Frequently, these transcription factors provide transient regulatory input, but a subset of them remains expressed during the lifetime of mature non-dividing β-cells (Holmberg & Perlmann, 2012; Szabat *et al*, 2012). In particular, Neurod1, Foxa1, Foxa2, Nkx6.1 and Pdx1 were first identified to control β-cell development but are now known to also maintain mature β-cell function (Naya *et al*, 1997; Ahlgren *et al*, 1998; Holland *et al*, 2002; Gao *et al*, 2007, 2010; Gu *et al*, 2010; Szabat *et al*, 2012; Taylor *et al*, 2013). This shows that the persistent and mature gene expression program in β-cells is actively controlled, but only recently the integration of these factors into regulatory networks is beginning to receive attention (Pasquali *et al*, 2014).

Maturity is known to be important for β-cell function, and loss of maturity was associated with failure of glucose-stimulated insulin secretion in diabetes (Weir & Bonner-Weir, 2004; Ziv *et al*, 2013; Wang *et al*, 2014). Insulin release is finely tuned and relies on mechanisms that allow β-cells to sense and metabolize glucose, as well as on signaling cascades that couple metabolic signals to insulin exocytosis (Lang, 1999; MacDonald *et al*, 2005). In addition to glucose as primary regulator, metabolites such as free amino acids or fatty acids also stimulate insulin secretion. Furthermore, hormones such as glucagon-like peptide-1 (Glp1) and gastrointestinal inhibitory polypeptide (GIP) modulate and serve as potentiators of glucose-induced insulin secretion (MacDonald *et al*, 2005; Baggio & Drucker, 2007). Thus, in a normal physiological setting in the adult, insulin secretion is controlled by glucose and additional signals that provide modulatory input. β-cells of adult and newborn mice differ in their response to these complex cues, indicating that the ability to appropriately

1 Developmental Biology, Max-Delbrück-Center for Molecular Medicine, Berlin, Germany
2 Systems Biology of Gene Regulatory Elements, Max-Delbrück-Center for Molecular Medicine, Berlin, Germany
3 Electron Microscopy Platform, Max-Delbrück-Center for Molecular Medicine, Berlin, Germany
4 Scientific Genomics Platform, Max-Delbrück-Center for Molecular Medicine, Berlin, Germany
5 Molecular Mechanisms of Metabolic Disease, Max-Delbrück-Center for Molecular Medicine, Berlin, Germany
*Corresponding author. Tel: +49 30 9406 2403; Fax: +49 30 9406 3765; E-mail: cbirch@mdc-berlin.de
**Corresponding author. Tel: +49 30 9406 3848; Fax: +49 30 9406 3765; E-mail: jshiqi@mdc-berlin.de
‡These authors contributed equally to this work
†Present address: Department of Medical Oncology, Jiangsu Provincial Hospital of TCM, Nanjing, China

secrete insulin is acquired during postnatal maturation. To restore β-cells or β-cell functions in diabetic patients, *in vitro* protocols were developed that allow the generation of β-cells from embryonic stem cells by a step-wise differentiation that recapitulates development *in vivo* (D'Amour *et al*, 2006; Nostro & Keller, 2012). Until recently, such methods yielded immature β-cells that poorly secrete insulin in response to glucose, but a new protocol was recently reported to overcome this limitation (Pagliuca *et al*, 2014). Despite the physiological importance of β-cell maturity, the maturation process remains little understood on a molecular level.

Insm1 encodes a zinc finger factor that controls differentiation of β-cells and other endocrine cell types in the pancreas, intestine, pituitary and adrenal medulla (Gierl *et al*, 2006; Wildner *et al*, 2008; Welcker *et al*, 2013; Osipovich *et al*, 2014). In endocrine cells of the pancreas, *Insm1* expression is initiated early during development in an Ngn3-dependent manner (Gierl *et al*, 2006; Mellitzer *et al*, 2006). *Insm1* but not *Ngn3* expression is maintained in mature endocrine cells, providing an example of the distinct regulatory cascades operative in development and maturity. We show here that Insm1 binds to chromatin in β-cells and that most Insm1 sites are co-occupied by two key β-cell transcription factors, Neurod1 and Foxa2. Using conditional gene ablation in mice, we show that *Insm1* controls mature β-cell function and is required for correct glucose-stimulated insulin secretion. Mutant β-cells shift their functional properties and gene expression program to resemble immature β-cells. Binding sites co-occupied by Insm1/Neurod1/Foxa2 are mainly located in intergenic and intronic sequences. Remarkably, the presence of such combinatorial binding sites correlates very significantly with gene expression changes in *Insm1* mutant β-cells. Conversely, sites occupied by Insm1 only are enriched in promoters and correlate poorly with gene expression changes. Together, our data provide evidence that combinatorial binding of Insm1, Neurod1 and Foxa2 identifies *cis*-regulatory sequences that maintain the mature gene expression program of β-cells.

Results

Insm1 ablation in mature β-cells abrogates glucose-stimulated insulin secretion

In the mature murine pancreas of control mice, nuclear Insm1 protein was detected by immunohistology in insulin$^+$ β-cells (Fig 1A and B). Other endocrine cell types like α-cells that express glucagon (Gcg), δ-cells that express somatostatin (Sst) and Pp-cells that express pancreatic polypeptide (Pp) locate to the periphery of murine islets and also express Insm1 (Fig 1C–E). In contrast to the expression observed in developing endocrine cells, Insm1 protein levels in adult endocrine cells appeared heterogeneous and β-cells that express high and low Insm1 levels were observed. To assess the role of *Insm1* in mature β-cell gene regulation and function, we introduced a somatic *Insm1* mutation in mice using a 'floxed' allele ($Insm1^{flox/lacZ}$; Supplementary Fig S1A and Materials and Methods) and a tamoxifen-inducible Cre driven by the insulin promoter (*RIPCreER*; Dor *et al*, 2004). To test for specificity of recombination using *RIPCreER*, the *mT/mG* indicator line was used that expresses membrane-bound tomato and GFP before and after Cre-dependent recombination, respectively (Muzumdar *et al*, 2007). After tamoxifen treatment of *mT/mG;RIPCreER* animals, the vast majority of insulin$^+$ cells co-expressed GFP, indicating that recombination is efficient in β-cells (Fig 1F and G). Non-recombined tomato$^+$ cells in islets were also observed (Fig 1H). These co-expressed PECAM, glucagon, pancreatic polypeptide and somatostatin (Fig 1I–L), indicating that recombination does not occur in endothelial, α-, δ- and Pp-cells. We used tamoxifen-treated mice with an $Insm1^{flox/lacZ}$*;RIPCreER* genotype as conditional mutants, which are subsequently called *coInsm1* mutants. In *coInsm1* mutants, a pronounced reduction of Insm1 protein was observed by immunohistology in insulin$^+$/Pdx1^{high} β-cells (Fig 1M–P) and by Western blot analysis of isolated islets (Fig 2A).

We next assessed plasma insulin levels in control and mutant mice. When insulin secretion was monitored after glucose injection in *coInsm1* mutants, we observed a completely disrupted insulin secretion; that is, insulin levels were not elevated 2, 5 or 15 min after the injection (Fig 2B). Insulin secretion was also impaired during a 2-h period after glucose challenge (Supplementary Fig S1B). In fasted *coInsm1* and control animals, insulin levels were similar (Fig 2C). We also monitored insulin levels in randomly fed animals that receive a mixture of nutrients, that is, under conditions in which insulin secretion is regulated by complex physiological parameters encompassing glucose, other nutrients and hormones. This showed that insulin levels were increased in randomly fed compared to fasted *coInsm1* mice (Fig 2C). However, insulin levels did not reach those observed in randomly fed control mice (Fig 2C). Blood glucose levels of randomly fed *coInsm1* animals were markedly elevated, and *coInsm1* mice showed pronounced elevation of blood glucose in glucose tolerance tests (Fig 2D and E). Elevated glucose levels were consistently observed in *coInsm1* mice 2–11 weeks after tamoxifen treatment (Fig 2F). Similar changes in glucose levels were observed in randomly fed and glucose challenged mice regardless whether the mutation was introduced at an age of 1 or 2 months (compare Fig 2D and E; Supplementary Fig S1C and D). In all experiments described above, we compared *coInsm1* mutants to control animals of two genotypes, $Insm1^{flox/+}$; *RIPCreER* and $Insm1^{flox/lacZ}$. Since the two control groups were indistinguishable, we combined them in subsequent experiments.

Insm1 is required for normal islet morphology and insulin content

We next tested whether decreased insulin release was caused by β-cell loss or reduced insulin production. Pancreatic β-cell numbers were comparable in control and mutant mice (Fig 3A), but β-cell mass was mildly reduced in the mutants (Fig 3B). Insulin content and insulin-1 (*Ins1*) but not insulin-2 (*Ins2*) mRNAs were mildly reduced in *coInsm1* mutant pancreata (Fig 3C and D). Mice that lack the insulin-1 gene remain glucose tolerant (Leroux *et al*, 2001), indicating that the mild downregulation of insulin-1 mRNA cannot account for the pronounced deficit in insulin secretion observed in *coInsm1* mutant mice.

Histological analyses showed that the average cell size was reduced resulting in denser nuclear packing, but overall epithelial cell morphology was intact as assessed by β-catenin distribution (Fig 3E). The smaller cell size can thus account for the reduction in the β-cell mass. TUNEL staining showed that apoptosis rates were elevated in islets of *coInsm1* mutants, but they nevertheless remained low (< 1 apoptotic cell/section; Fig 3F). This was

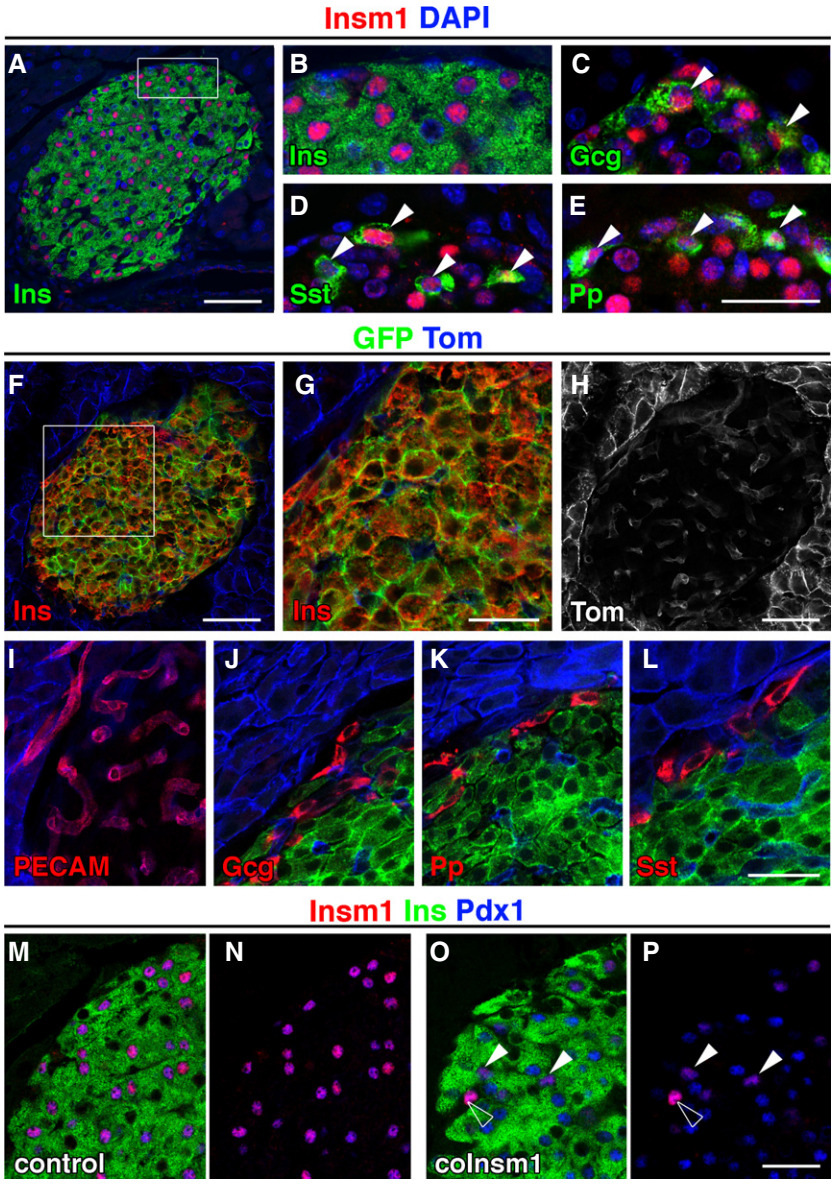

Figure 1. Insm1 is expressed in adult pancreatic endocrine cells, and RIPCreER induces efficient and β-cell-specific mutation of Insm1.

A–E Analysis of Insm1 protein (red) in pancreata of adult control mice by immunohistology, using DAPI (blue) as counterstain. Insm1 is present in (A, B) β-cells that express insulin (Ins, green), (C) α-cells that express glucagon (Gcg, green), (D) δ-cells that express somatostatin (Sst, green) and (E) Pp-cells that express pancreatic polypeptide (Pp, green). Arrowheads indicate cells co-expressing Insm1 and Gcg (C), Insm1 and Sst (D), Insm1 and Pp (E).

F–L Analysis of *RIPCreER*-induced recombination using *mT/mG* reporter mice that express membrane-bound tomato and GFP before and after Cre-mediated recombination, respectively. The insulin$^+$ β-cells co-express GFP and have thus undergone recombination. Cells that express tomato co-express PECAM, glucagon, pancreatic polypeptide or somatostatin and are thus not recombined.

M, N Co-localization of Insm1 and Pdx1 in nuclei of insulin$^+$ β-cells in control mice.

O, P Insm1 protein is lost in most β-cells of *coInsm1* mice. Arrowheads indicate remaining un-recombined β-cells that continue to express Insm1; the open arrowhead points towards an Insm1$^+$ endocrine cell that does not co-express insulin.

Data information: Scale bars: 50 μm (A, F, H); 25 μm (E, G, L, P).

accompanied by a mild increase in proliferation (Fig 3G). We also found that glucagon-expressing α-cells were increased in number and dispersed throughout the islet instead of being located in the periphery (Fig 3H). The numbers and locations of somatostatin- and pancreatic peptide-expressing cells and expression of other hormones were unchanged (Supplementary Fig S2). In conclusion, ablation of Insm1 in adult β-cells resulted in perturbed islet morphology, reduced β-cell mass due to smaller cell volume and decreased pancreatic insulin content.

Insm1 mutant β-cells assume immature functional characteristics

We next tested systematically for changes in gene expression in *coInsm1* mutant islets by microarray analysis (GSE54044), which

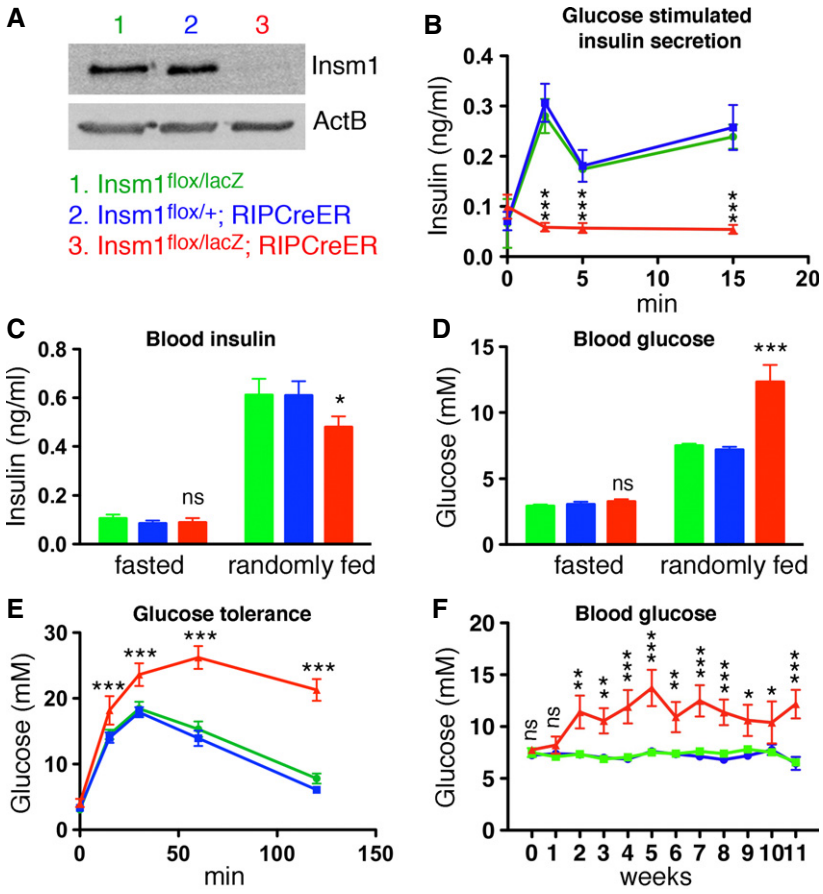

Figure 2. Conditional mutation of Insm1 results in disrupted glucose-stimulated insulin secretion and glucose intolerance.

A Western blot analysis of Insm1 in isolated islets of control and *coInsm1* mutant mice (pool of 200 islets from 2 to 3 mice).

B Glucose-stimulated insulin secretion in control and *coInsm1* mice. The mice were injected with glucose at $t = 0$, and insulin secretion was monitored over time ($n = 12–14$).

C Blood insulin levels in fasted and randomly fed control (green bars: *Insm1*$^{flox/lacZ}$; blue bars: *Insm1*$^{flox/+}$;*RIPCreER*) and *coInsm1* mice (red bars: *Insm1*$^{flox/lacZ}$;*RIPCreER*) ($n = 14–16$).

D Blood glucose levels in fasted and randomly fed control and *coInsm1* mice; mutations were introduced at an age of 4–5 weeks, and mice were analyzed at 8–12 weeks. Glucose levels in mutant mice were 12.3 ± 1.3 mM (range of 4.0–24.7 mM), in contrast to 7.5 ± 0.2 mM and 7.2 ± 0.2 mM (range of 6.0–10.2 mM) in control mice ($n = 12–14$).

E Glucose tolerance test in control and *coInsm1* mice ($n = 12–14$).

F Blood glucose levels in randomly fed control and *coInsm1* mice at various time points (0–11 weeks) after introduction of the mutations ($n = 12–14$).

Data information: Data are presented as means ± SEM, statistical significance was assessed by ANOVA and 2-tailed unpaired Student's *t*-test. *$P < 0.05$; **$P < 0.01$; ***$P < 0.001$.
Source data are available online for this figure.

revealed deregulated genes in mutant islets (P-value < 0.05; 1,232 genes with FC > 1.2 and < 0.8; 352 with FC > 1.4 and < 0.6). Similar numbers of genes were up- and down-regulated. To define affected cellular processes, we performed Gene Ontology (GO) term analysis of differentially expressed genes. Consistent with glucose intolerance, deregulated genes were associated with biological processes critical for β-cell function, such as regulation of insulin secretion, response to hormone and glucose stimulus, and glucose metabolism (Fig 4A; Supplementary Table S1). Comparison with *Insm1*-dependent genes identified previously in the developing pancreas (Gierl *et al*, 2006) revealed little overlap (61 overlapping genes, Pearson's coefficient 0.21, Supplementary Table S2). Thus, Insm1 controls distinct sets of genes in developing and mature β-cells.

Insulin exocytosis from pancreatic β-cells is stimulated by glucose metabolism by a mechanism involving ATP-sensitive K^+ channels (MacDonald *et al*, 2005). In addition, hormones such as glucagon-like peptide-1 (Glp1) and gastrointestinal inhibitory polypeptide (GIP) and metabolic fuels potentiate insulin secretion (Baggio & Drucker, 2007). Many deregulated genes identified participate in glucose-dependent insulin secretion, such as *Glut2* (*Slc2a2*), *Pcx*, *Pfkfb3*, *Hk1*, *Pdk1/4* and *G6pc2* that control glucose uptake and metabolism, a subunit of the ATP-sensitive potassium channel (*Abcc8*), intracellular signaling molecules (*Prckb*, *Ak5*, *Trpm5*, *Cx36*), glucagon-like peptide-1 receptor (*Glp1r*) and a negative regulator of GIP receptor signaling (*Rgs2*) (see Supplementary Table S1 for a list of deregulated genes implicated in insulin secretion;

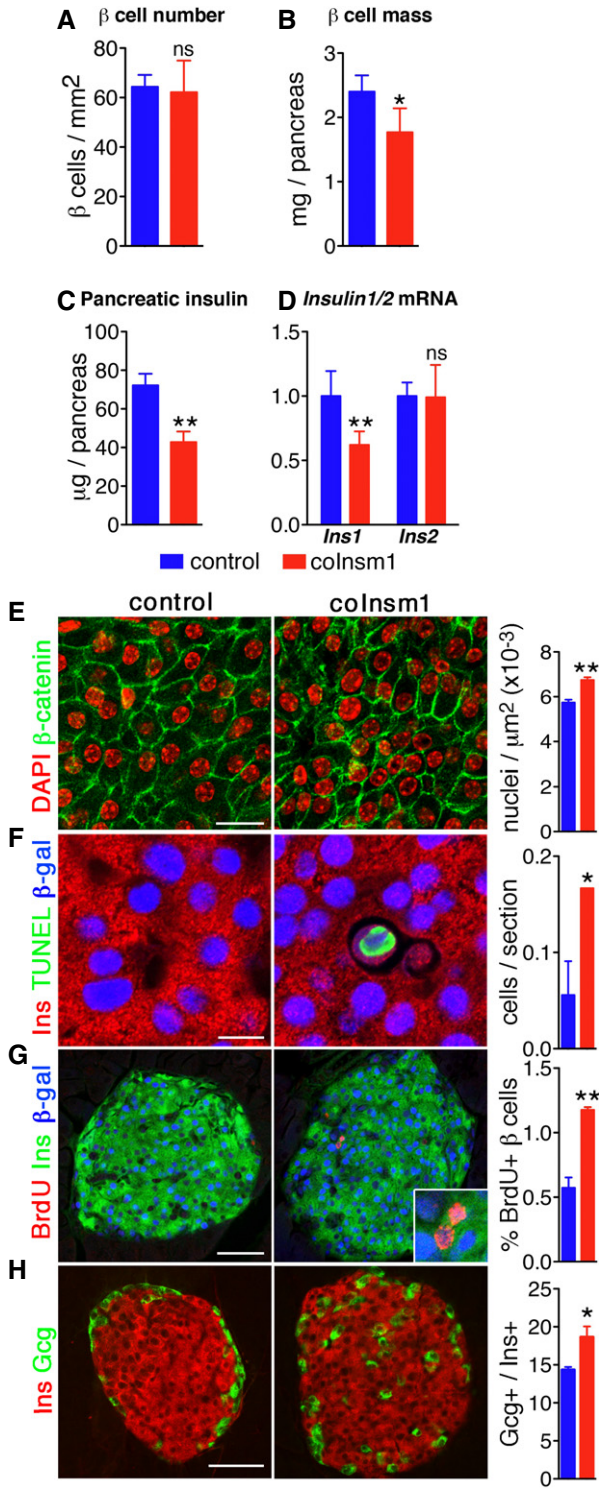

Figure 3. Altered islet morphology in *coInsm1* mutant mice.

A, B Comparison of β-cell number (A) and β-cell mass (B) in control and *coInsm1* mice (n = 3 mice, 6–8 slides/animal). The number given in (A) refers to cell numbers/pancreas area.

C, D Total pancreatic level of insulin (n = 6–12) (C) and *Ins1* and *Ins2* mRNA in control and *coInsm1* mice (n = 5) (D).

E Epithelial morphology and quantification of the packing density of islet cells in control and *coInsm1* mice. The number given refers to cell numbers/islet area.

F Analysis of cell death in β-cells of control and *coInsm1* mice by TUNEL staining.

G Comparison of proliferation in islets of control and *coInsm1* mice using BrdU incorporation.

H Distribution and quantification of glucagon$^+$ cells in pancreata of control and *coInsm1* mice.

Data information: Data are presented as means ± SD; statistical significance was assessed by ANOVA and 2-tailed unpaired Student's t-test. *$P < 0.05$; **$P < 0.01$. (A, B, E–H) n = 3. Scale bars: 20 µm (E); 10 µm (F); 50 µm (G, H).

Babenko *et al*, 2006; Becker *et al*, 1994; Carvalho *et al*, 2010; Colsoul *et al*, 2010; Guillam *et al*, 1997; Stanojevic *et al*, 2008; Sugden & Holness, 2013; Tseng & Zhang, 1998; Wang *et al*, 2007; Xu *et al*, 2008). The expression of deregulated genes implicated in insulin secretion was confirmed by qRT–PCR (Fig 4B). Ucn3 provides a marker for β-cell maturity, and the ratio of MafB and MafA expression is important during β-cell maturation (Artner *et al*, 2010; Blum *et al*, 2012; van der Meulen *et al*, 2012; Hang *et al*, 2014). We also observed that *Ucn3*, *MafB* and *MafA* were deregulated in *coInsm1* mutant islets. This provided first evidence that *coInsm1* mutant islets have lost a mature gene expression program.

We therefore systematically compared genes deregulated in *coInsm1* islets to previously reported genes differentially expressed in mature and immature (P1) murine β-cells (Blum *et al*, 2012; GSE35906). This revealed a large overlap; that is, 29% of the genes that were differentially expressed in control and *coInsm1* mutant islets were also differentially expressed in mature and immature β-cells; a hypergeometric probability test demonstrated that this overlap was highly significant ($P < 5.6 \times 10^{-9}$; Fig 4C). We also compared the differentially expressed genes of *coInsm1* mutants with a diabetes model (Kluth *et al*, 2014) and found a more limited overlap (115 genes deregulated in both models, $P = 1$). Islets of *coInsm1* mutants resemble thus more closely immature than diabetic islets. *Ucn3*, *Glut2* and *Glp1r* were among the common set of deregulated genes in immature and *coInsm1* mutant islets, and Western blotting demonstrated reduced levels of the corresponding proteins (Fig 4D). *Ngn3* and other markers of β-cell progenitors were not induced (Supplementary Fig S3). This indicates that *coInsm1* mutant β-cells revert to an immature but not progenitor state.

Immature β-cells, for instance those from newborn mice, are known to respond aberrantly to glucose (Rorsman *et al*, 1989; Blum *et al*, 2012). We therefore characterized and directly compared glucose-induced insulin secretion from islets isolated from *coInsm1* mutants and immature mice (Fig 4E and F). *coInsm1* mutant but not control islets released insulin at 3.3 mM glucose, but glucose-stimulated insulin release was similar at 16.7 mM. In control islets, insulin secretion was further enhanced by pyruvate, exendin-4 and GIP in the presence of 16.7 mM glucose, but *coInsm1* mutant islets responded poorly to these secretagogues (Fig 4E). Similar changes in insulin secretion were observed in immature islets obtained from postnatal day 1 (P1) mice, that is, increased insulin release at low glucose (3.3 mM) and poor response to pyruvate, exendin-4 and GIP (Fig 4F). *coInsm1* mutant islets and immature islets also displayed a similar decrease in sensitivity to tolbutamide, a blocker of ATP-sensitive potassium channels (Fig 4E and F). Stimulation with KCl released similar amounts of insulin from control, *coInsm1* mutant and from immature islets (Fig 4E and F). This indicated that the overall secretory machinery remained functional in *coInsm1* and immature islets. This was also supported by electron micrograph

Published online: March 31, 2015
The EMBO Journal

A

GO term	P value	Numbers of genes
regulation of secretion	$1.85x10^{-11}$	45
regulation of insulin secretion	$4.43x10^{-10}$	20
carbohydrate metabolic process	$5.86x10^{-10}$	43
hormone secretion	$5.84x10^{-9}$	26
hexose metabolic process	$1.18x10^{-8}$	27
ion homeostasis	$3.96x10^{-7}$	42
regulation of cell differentiation	$2.91x10^{-6}$	42
response to hormone stimulus	$3.00x10^{-6}$	35
glucose metabolic process	$5.60x10^{-6}$	20
small GTPase mediated signal transduction	$7.65x10^{-6}$	39
response to glucose stimulus	$1.76x10^{-5}$	12

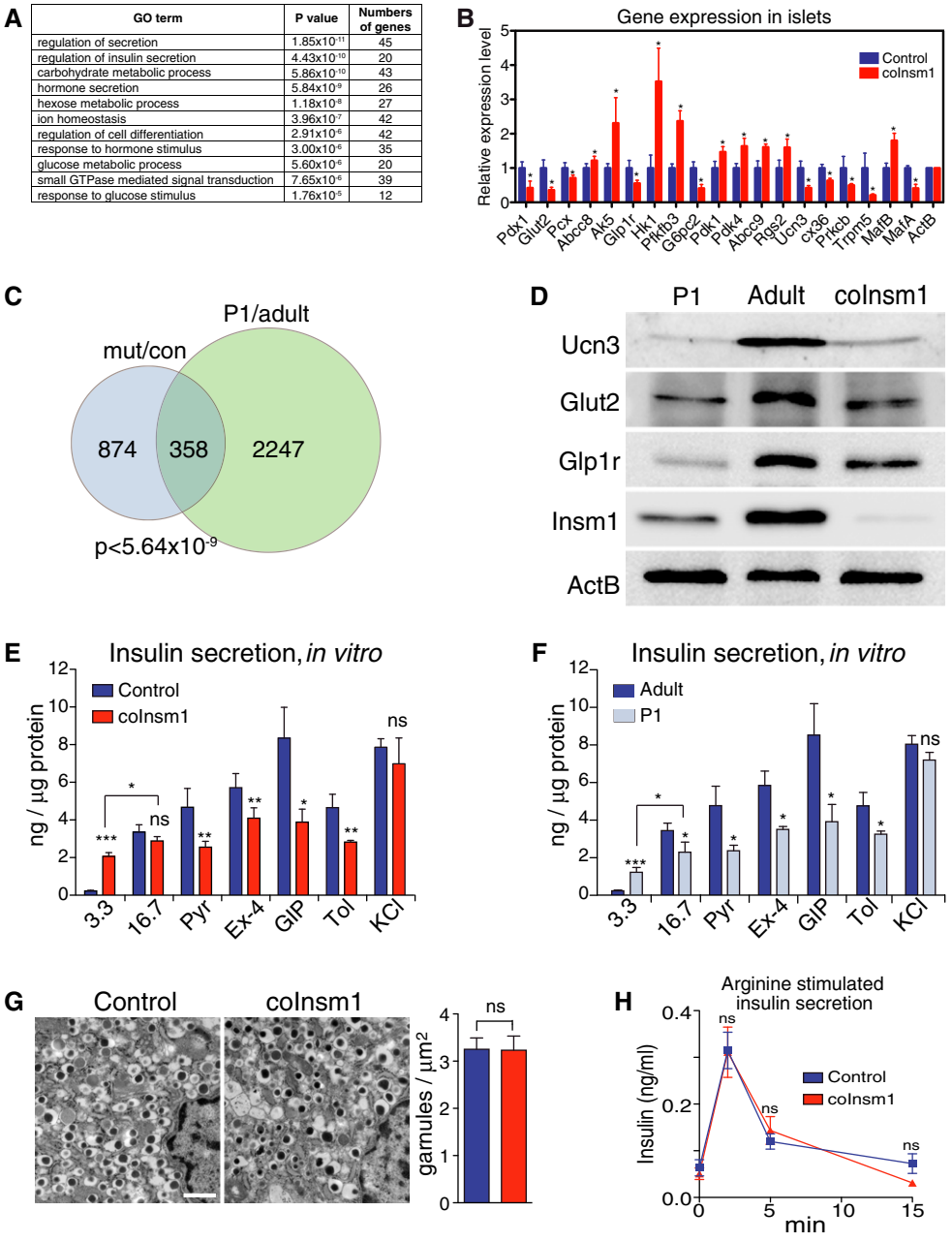

Figure 4. Mutation of *Insm1* disrupts mature gene expression in adult islets.

A GO term analysis of differentially expressed genes identified by microarray analysis in isolated islets from control and *coInsm1* mutant mice. Shown are GO terms, the *P*-value for their enrichment and the number of differentially expressed genes associated with a particular GO term.

B Verification of differential expression of genes previously implicated in the control of insulin secretion; RNA from isolated islets of control and *coInsm1* mutant mice was compared by qRT–PCR (n = 5).

C Comparison of the deregulated genes identified in *coInsm1* mutant versus control islets and sorted β-cells from P1 and adult mice. 1,232 genes were differentially expressed in *coInsm1* mutant islets, and among these, 358 were previously identified as differentially expressed in immature versus mature β-cells.

D Analysis of Ucn3, Glut2 and Glp1r protein by Western blotting; a representative of three experiments is shown.

E Insulin secretion from isolated islets of control and *coInsm1* mutant mice in response to glucose (3.3 and 16.7 mM), and in response to 16.7 mM glucose and additional secretagogues, that is, 100 mM pyruvate (Pyr), 20 nM exendin-4 (Ex-4), 100 nM gastric inhibitory polypeptide (GIP), 200 µM of the ATP-sensitive K^+ channel inhibitor tolbutamide (Tol) and in response to membrane depolarization (30 mM KCl) (n = 3–4).

F Insulin secretion from isolated islets of P1 and adult mice in response to glucose, secretagogues and membrane depolarization (n = 3–4).

G Secretory vesicle appearance and density in control and *coInsm1* mutant β-cells (n = 3).

H Arginine-induced insulin secretion was intact in *coInsm1* mutant mice (n = 6–15).

Data information: Data are presented as means ± SD; statistical significance was assessed by ANOVA and 2-tailed unpaired Student's *t*-test. *$P < 0.05$; **$P < 0.01$; ***$P < 0.001$. Scale bar: 1 µm.
Source data are available online for this figure.

analysis of insulin-containing secretory granules in β-cells that did not reveal changes in vesicular morphology or density in mutant mice (Fig 4G). Furthermore, examination of arginine-induced insulin secretion *in vivo* did not reveal significant differences between control and *coInsm1* animals (Fig 4H). Thus, mutant β-cells remain fully capable of insulin secretion after challenge with arginine *in vivo* or by global membrane depolarization by exogenous KCl *in vitro*. In summary, the primary deficit in *coInsm1* mutant β-cells is restricted to glucose-induced insulin secretion and its modulation by secretagogues, excluding a general deficit in the basic secretory machinery. This is also supported by the fact that genes controlling glucose sensing and metabolism, secretagogue response and intracellular signaling are deregulated.

Insm1 binds to chromatin cooperatively with Neurod1 and Foxa2

To understand the molecular mechanism of Insm1 function in β-cells, ChIP-seq experiments were performed. As a chromatin source, we used early passages of an immortalized pancreatic β-cell line (referred to as SJ β-cells) that we established (Radvanyi *et al*, 1993). Insulin secretion from SJ β-cells was stimulated eightfold to tenfold in response to glucose, which is comparable to the response observed in dissociated cells from adult islets, but lower than the one in intact islets, and these cells respond to exendin-4 and GIP (Supplementary Fig S4A; compare with Blum *et al*, 2012; Halban *et al*, 1982). Two independent ChIP-seq experiments (GSE54046) identified 17,453 high confidence Insm1 binding sites in chromatin of SJ β-cells that overlapped between experiments (see Supplementary Fig S4B–D for replicate comparisons, antibody specificity and binding site distribution). Example traces are shown in Fig 5A and Supplementary Fig S4E (upper traces). Examination of these binding sites by *de novo* motif analyses revealed an enrichment of two sequences within ±25 bp of the summits of binding sites (Fig 5Bi and ii; E-value = 8×10^{-92} and 8×10^{-41} for the two motifs shown in i and ii, respectively). The first corresponds to an E-box (present in 22% of all Insm1 binding sites) and the second to the consensus sequence of forkhead factors (present in 21% of all Insm1 binding sites; Newburger & Bulyk, 2009). The previously described consensus Insm1 binding sequence (Breslin *et al*, 2002) was not identified by *de novo* motif analysis, but a related sequence (Fig 5B iii) was observed in 19% of all Insm1 binding sites (E-value = 5.5×10^{-55}; see also below).

The key β-cell transcription factors Neurod1 and Foxa2 bind E-box and forkhead motifs, respectively. We tested whether Neurod1 and Foxa2 co-occupy Insm1 sites in β-cell chromatin using ChIP-seq analysis. A total of 14,607 Neurod1 and 28,379 Foxa2 binding sites were identified in the genome of SJ β-cells; 38% of the Neurod1 and 46% of the Foxa2 sites contained the known E-box and forkhead consensus motif, respectively, within ±25 bp of the summit of the peaks. Binding sites of Insm1 in the genome displayed large degrees of overlap with Neurod1 and Foxa2: 73% of all Insm1 sites were co-occupied by Neurod1 and/or Foxa2, and 38% were co-occupied by all three factors (Fig 5C). Summits of single factor binding peaks were typically close and less than 50 bp apart (Fig 5D). Traces for all three factors are shown for the key β-cell transcription factor *Pdx1* and the glucose transporter *Glut2* (*Slc2a2*) (Fig 5A), as well as for *Ucn3*, *Ins1*, hexokinase1 (*Hk1*) and *MafA* (Supplementary Fig S4E; see also Supplementary Table S3). Many Insm1 sites not classified as Neurod1 or Foxa2 binding sites nevertheless displayed substantial Neurod1 or Foxa2 coverage that had not sufficed to pass the stringent cutoff (Fig 5E, Materials and Methods). We also performed *de novo* motif analyses on co-occupied and 'Insm1 only' sites. In 'Insm1 only' sites, two motifs were identified, one resembling the described Insm1 consensus sequence (Fig 5B iiii) (Breslin *et al*, 2002) and the second corresponding to a new motif (Supplementary Fig S5); neither of these were identified in sites co-occupied by all three factors.

Next, we compared the number of reads obtained in Insm1, Neurod1 or Foxa2 ChIP-seq experiments and observed that read numbers were highest at sites co-occupied by all three factors (Fig 6A). Comparison of the distribution of co-occupied and 'Insm1 only' sites in the genome demonstrated that co-occupied sites were depleted of promoter and enriched in intergenic and intronic sequences (Fig 6B). The co-recruitment of Insm1, Neurod1 and Foxa2 was also experimentally tested by ChIP-PCR in both SJ β-cells and murine islets. Indeed, all tested sites were enriched (Fig 6C and D). Thus, Insm1, Neurod1 and Foxa2 frequently bind in close proximity in chromatin of pancreatic β-cells, and high affinity binding sites are enriched in sites co-occupied by all three factors.

We next tested whether Insm1 and Neurod1 and/or Foxa2 bind simultaneously or competitively by sequential chromatin immunoprecipitation (ChIP-reChIP) (Truax & Greer, 2012). After precipitation of chromatin from SJ β-cells and murine islets by anti-Insm1 antibodies, we observed substantial re-precipitation with anti-Neurod1 or anti-Foxa2 antibodies (Fig 7A–D). Thus, Insm1/Neurod1 and Insm1/Foxa2 can bind simultaneously. We also tested whether Insm1 directly interacts with Neurod1 or Foxa2 using immunoprecipitation and Western blotting. Anti-Insm1 antibodies co-precipitated endogenous Neurod1, and to a lesser extend Foxa2 in SJ β-cells (Fig 7E). Co-precipitation was also observed in the presence of ethidium bromide (Fig 7E), indicating that Insm1/Neurod1 and Insm1/Foxa2 interactions are independent of DNA binding (Lai & Herr, 1992). Conversely, the endogenous Insm1 was immunoprecipitated by anti-Neurod1 and anti-Foxa2 antibodies in the presence and absence of ethidium bromide, but not by control or anti-MafA antibodies (Fig 7E). Thus, Insm1 physically interacts strongly with Neurod1, and to a lesser extent with Foxa2, indicating that Insm1 can be recruited also indirectly to chromatin.

We chose sequences to assess them for enhancer activity in β-cells (SJ cells), hepatocytes (HepG2 cells) and a kidney cell line (HEK293) by luciferase assays. Sequences chosen were associated with deregulated genes and either co-occupied by Insm1/Neurod1/Foxa2 (indicated by 3 in Fig 7F), by other combinations of Insm1 sites (indicated by 2) or by Insm1 only (indicated by 1). The majority of Insm1/Neurod1/Foxa2 co-occupied sites were more active in β-cells than in HepG2 or HEK293 cells (Fig 7F). Thus, sites that integrate binding of all three factors display *cis*-regulatory activity and β-cell lineage selectivity. Indeed, Insm1/Neurod1/Foxa2 sites were strongly enriched in the previously characterized putative enhancers of β-cells (Supplementary Table S4; Tennant *et al*, 2013). Six fragments that displayed lineage-specific regulatory activity were further analyzed by luciferase assays in HepG2 cells that express endogenous *Foxa2*, but not *Insm1* or *Neurod1*. *Insm1* or *Neurod1* cDNA was transfected together with luciferase constructs. Expression of *Neurod1* cDNA but not of *Insm1* cDNA alone stimulated transcriptional activity of enhancer fragments from the

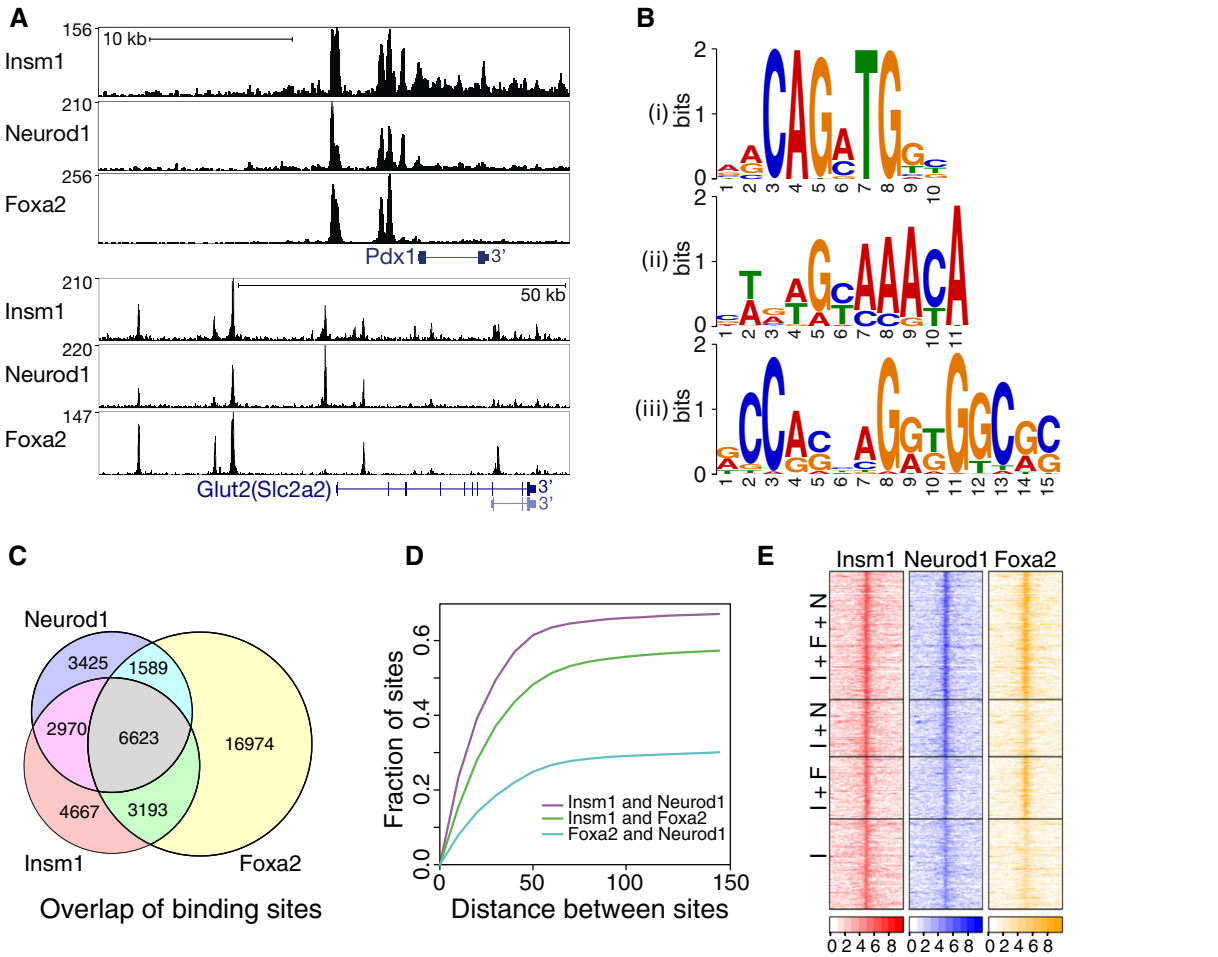

Figure 5. Insm1 binds chromatin sites that are co-occupied by Neurod1 and Foxa2.

A Insm1, Neurod1 and Foxa2 ChIP-seq binding tracks identified in chromatin from SJ β-cells for *Pdx1* and *Glut2* (*Slc2a2*).

B *De novo* motif analysis of Insm1 peaks identified consensus binding sequences of basic helix-loop-helix and forkhead factors (i and ii); in addition, an Insm1 motif (iii) identified in 'Insm1 only' sites that resembles the known Insm1 binding sequence is shown.

C Overlap between Insm1, Neurod1 and Foxa2 binding sites.

D Distance between the summits of Insm1 and Neurod1 (violet), Insm1 and Foxa2 (green) as well as Foxa2 and Neurod1 (light blue) peaks; displayed are the fraction of peaks versus the distance between binding sites in base pairs.

E Heat map showing read tracks for Insm1, Neurod1 and Foxa2 at sites co-occupied by Insm1/Neurod1/Foxa2 (I+F+N; top), Insm1/Neurod1 and Insm1/Foxa2 (I+N and I+F; middle), or at sites bound by Insm1 only (I; bottom). The color code indicates read density ±2 kb around binding sites as log2 of the number of reads.

Glp1r and *Pcx* genes. Remarkably, *Neurod1* and *Insm1* co-transfection stimulated expression synergistically (Fig 7G), which was observed with enhancer fragments from *Glp1r* and *Pcx* genes but not other tested fragments. We conclude from these data that Neurod1 and Insm1 can act synergistically to increase transcriptional activity.

Combinatorial Insm1/Neurod1/Foxa2 binding sites correlate with Insm1-dependent gene regulation

Transcription factors typically bind to many thousand sites in the genome. It has remained a challenge to identify among these sites the ones functionally important for regulating gene expression. We related Insm1 binding and changes in gene expression in *coInsm1* mutant islets. In comparison to all expressed genes, combinatorial Insm1/Neurod1/Foxa2 binding sites were significantly enriched in deregulated genes (P-value = 2.2×10^{-19} and 8.0×10^{-22} for sequences 10 kb or 50 kb around the genes, respectively, for FC > 1.2). For instance, 16% of all expressed genes and 32% of deregulated genes (FC > 1.4) contained an Insm1/Neurod1/Foxa2 binding site within 10 kb (P-value = 4.3×10^{-13}). Sites occupied by 'Insm1 only' did not correlate with changed gene expression (Fig 8A). Additional computational analysis of other categories of single and combinatorial binding sites confirmed that sites co-occupied by Insm1/Neurod1/Foxa2 correlate best with changes in Insm1-dependent gene expression (Supplementary Table S5). Similar numbers of genes associated with Insm1/Neurod1/Foxa2 binding sites were up- and down-regulated (Supplementary Table S6), indicating that these sites regulate transcription in a context-dependent manner to activate or repress genes. Many deregulated genes associated with combinatorial Insm1/Neurod1/Foxa2 binding sites participate in insulin secretion, among them all deregulated genes whose expression was verified by qPCR in Fig 3B (see Supplementary Table S3 for a list

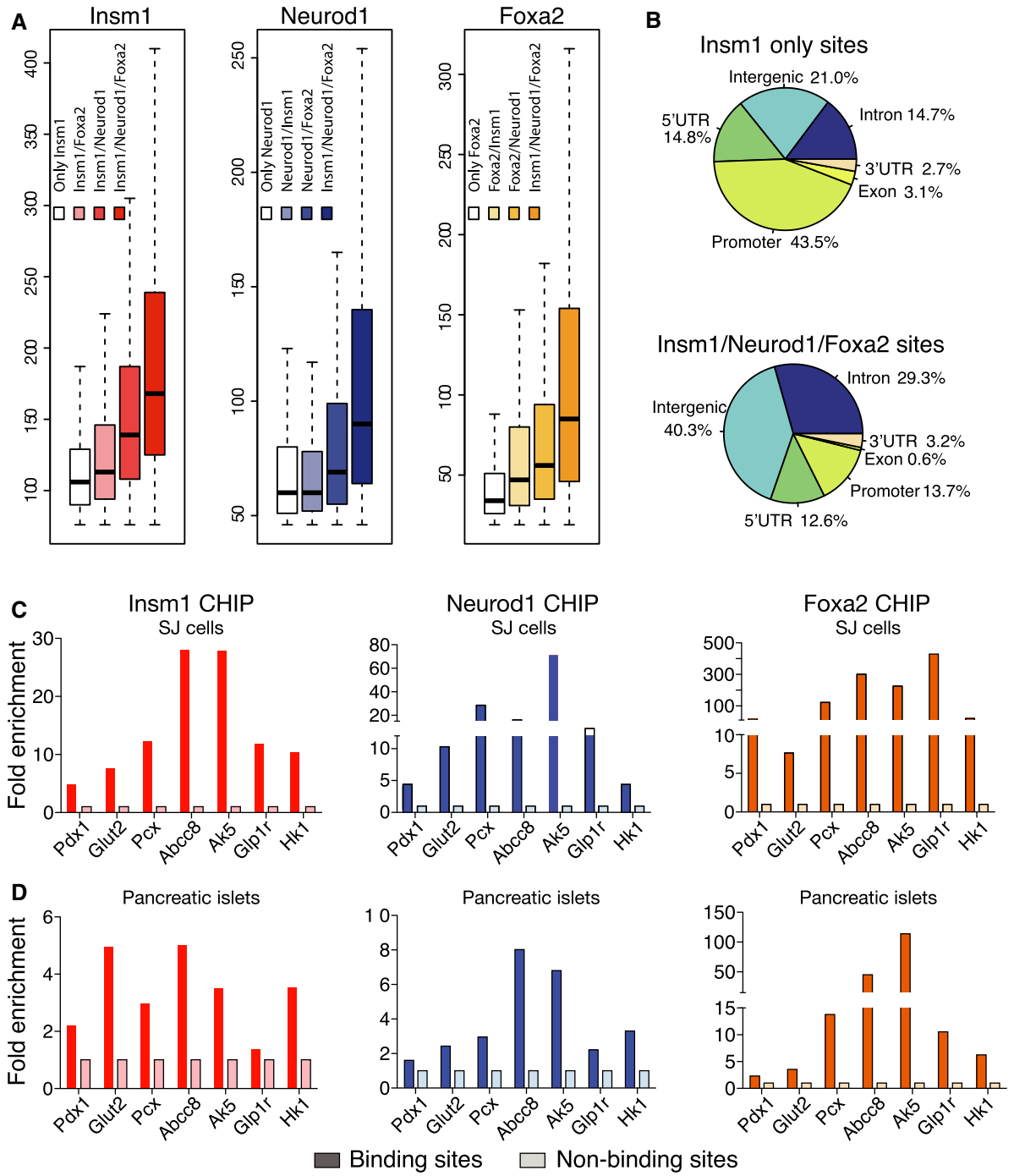

Figure 6. Sites co-occupied by Insm1, Neurod1 and Foxa2 correspond to high affinity sites and are enriched in intergenic and intronic sequences.

A Peak heights at sites occupied by individual factors, factor combinations and Insm1/Neurod1/Foxa2; median value (black line), quartiles (boxes) and errors (dashed lines) are shown (R package). Peak heights are largest at Insm1/Neurod1/Foxa2 sites ($P < 2.2 \times 10^{-16}$).

B Pie charts showing the distribution of Insm1 only sites (top) and Insm1/Neurod1/Foxa2 sites (bottom).

C, D ChIP-PCR analyses of Insm1, Neurod1 and Foxa2 binding in chromatin from SJ β-cells and isolated islets. Shown is the enrichment of precipitated chromatin; representative examples of three experiments are shown.

of deregulated genes implicated in insulin secretion associated with Insm1/Neurod1/Foxa2 sites). Finally, we defined the presence of Insm1/Neurod1/Foxa2 binding sites in genes deregulated in both, immature islets and *coInsm1*, and observed again a significant enrichment (P-value = 1.0×10^{-10} and 4.2×10^{-15} for sequences 10 kb and 50 kb around deregulated genes, respectively). We conclude that the presence of sites characterized by triple Insm1/Neurod1/Foxa2 binding is a predictor of Insm1-dependent gene expression.

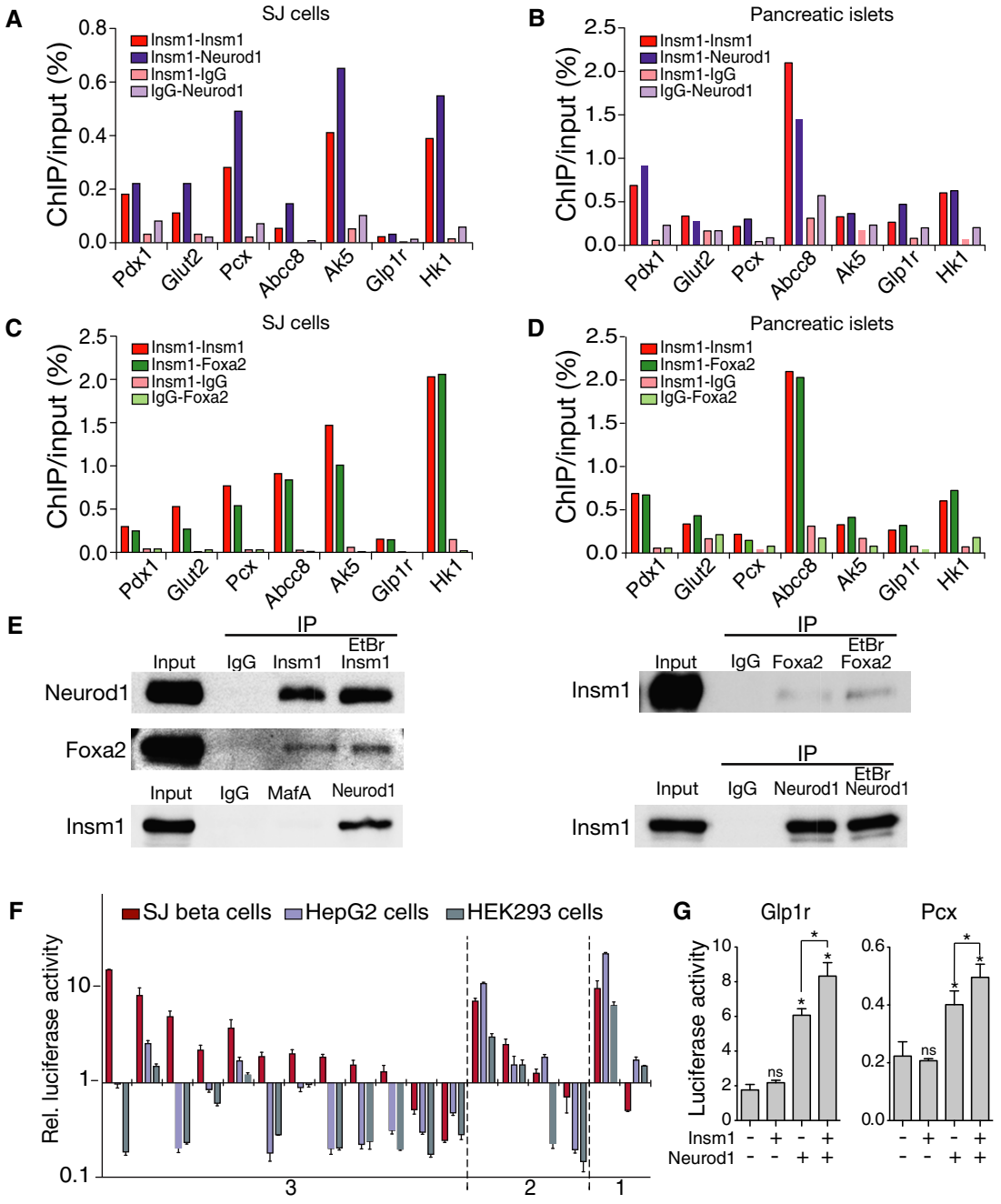

Figure 7. Direct interaction of Insm1, Neurod1 and Foxa2.

A reChIP-PCR analysis of selected binding sites in chromatin from SJ β-cells using antibodies against Insm1, Neurod1 and control IgG. Displayed is the percentage of the re-precipitated chromatin divided by chromatin input.

B reChIP-PCR analysis of chromatin from isolated islets using antibodies against Insm1, Neurod1 and control IgG. Displayed is the percentage of the re-precipitated chromatin divided by chromatin input.

C reChIP-PCR analysis of chromatin from SJ β-cell using antibodies against Insm1, Foxa2 and control IgG.

D reChIP-PCR analysis of chromatin from isolated islets using antibodies against Insm1, Foxa2 and control IgG.

E Co-immunoprecipitation of Insm1 and Neurod1, Insm1 and Foxa2 (but not Insm1 and MafA) in the presence or absence of ethidium bromide (EtBr). IP: antibody used for immunoprecipitation. The antibody used for Western blotting is also indicated. Representative results from one of three experiments are shown

F Luciferase reporter assay for *cis*-regulatory activity of DNA fragments associated with deregulated genes and Insm1 binding sites; luciferase reporter assays were performed in SJ β-cells, HepG2 and HEK293 cells. *y*-axis: luciferase activity relative to that of a plasmid with minimal promoter (pGL4-minP). *x*-axis: DNA regions co-occupied by Insm1/Neurod1/Foxa2 (category 3), Insm1/Neurod1 or Insm1/Foxa2 sites (category 2), or 'Insm1 only' (category 1) ($n = 4$).

G Synergistic transcriptional activation of fragments from the *Glp1r* and *Pcx* genes by Neurod1 and Insm1 in HepG2 cells ($n = 4$); *$P < 0.05$.

Data information: (A–D) Representative results from experiments done in triplicate (A, C) and duplicate (B, D) are shown. Data in (F, G) are presented as means ± SEM.
Source data are available online for this figure.

A

	Genes	Module within 10kb	Module within 50kb
Insm1/ Neurod1/ Foxa2 triple sites	All	16%	31%
	FC>1.2	26% ***	43% ***
	FC>1.4	32% ***	50% ***
Insm1 only sites	All	28%	46%
	FC>1.2	30% NS	45% NS
	FC>1.4	29% NS	45% NS

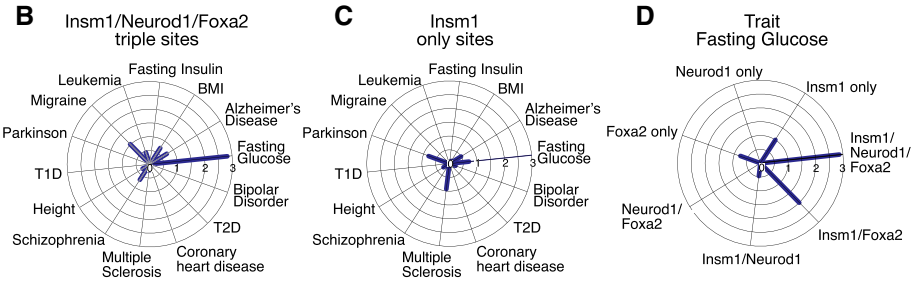

Figure 8. Sites co-occupied by Insm1, Neurod1 and Foxa2 correspond to a functionally important subclass of Insm1 sites.

A Proportions of all expressed and deregulated genes containing sites bound by Insm1/Neurod1/Foxa2 within ±10 kb and ±50 kb of the transcription start site (left). Proportions of all expressed and deregulated genes with sites occupied by Insm1 only ±10 kb and ±50 kb of the transcription start site (right). *P*-values for the enrichment of genes are indicated. NS: *P*-value > 0.01; ****P*-value ≤ 10^{-10}.

B, C SNPs with genome-wide association for 14 traits in European individuals overlapping with Insm1/Neurod1/Foxa2 and Insm1 only sites; note that SNPs associated with fasting glucose levels are significantly enriched in Insm1/Neurod1/Foxa2 but not in sites bound by Insm1 only.

D SNPs with genome-wide association for glycolytic traits in European individuals that overlap with different combinations of Insm1, Neurod1 and Foxa2 binding sites; *P*-values are displayed as −log10 values. Thus, SNPs associated with Insm1/Neurod1/Foxa2 binding sites are highly enriched for glycolytic traits.

Trait-associated variations in the genome (e.g., single nucleotide polymorphisms, SNPs) are often enriched in regulatory sequences (Hnisz *et al*, 2013; Pasquali *et al*, 2014). We defined human sequences that correspond to the experimentally identified Insm1 binding sites in mice and correlated them with known trait-associated variations. First, we examined SNPs obtained from the National Human Genome Research Institute (NHGRI) GWAS catalogue and included 14 traits, including traits associated with β-cell dysfunction such as diabetes, changed insulin and glucose levels. The most pronounced enrichment was observed for sites co-occupied by Insm1/Neurod1/Foxa2, and this was observed in SNPs associated with 'glucose levels', but sites occupied by 'Insm1 only' were not enriched (Fig 8B and C). Enrichment of other site categories or trait categories did not reach this level of significance (Fig 8D; Supplementary Table S7 for 98 combinations of binding site categories and their enrichment in SNPs associated with various traits). Several SNPs associated with type 2 diabetes were also located in Insm1/Neurod1/Foxa2 sites, but these were not significantly enriched. To further examine sequence variations, we also included SNPs identified in the largest available genome-wide association analyses for glycolytic traits (Morris *et al*, 2012; Scott *et al*, 2012) and again observed a significant enrichment of Insm1/Neurod1/Foxa2 sites (SNPs overlapping with Insm1/Neurod1/Foxa2 sites are listed in Supplementary Table S8). Thus, combinatorial Insm1/Neurod1/Foxa2 binding sites are enriched for sequences implicated in β-cell dysfunction in humans.

Discussion

Functional immaturity was associated with failure of pancreatic β-cells in disease (Weir & Bonner-Weir, 2004; Dor & Glaser, 2013; Wang *et al*, 2014). However, mechanisms that allow the acquisition and maintenance of the mature β-cell state are incompletely understood. We show here that Insm1 is required in adult β-cells to maintain the mature gene expression program. Conditional Insm1 ablation in mature β-cells leads to pronounced deficits in insulin secretion and to glucose intolerance, and mutant islets from adult mice resemble in these functional properties β-cells isolated from newborn animals. We used cultured cells as a model to analyze molecular mechanisms of Insm1 function and found that Insm1 binds to defined domains in chromatin that are mostly co-occupied by Neurod1 and Foxa2. Indeed, the presence of sites co-occupied by the three transcription factors correlates significantly with gene expression changes observed in *Insm1* mutant islets. Together, our data identify Insm1 as a component of an important transcriptional network that controls the gene expression program of mature pancreatic β-cells.

Functional interactions between Insm1, Neurod1 and Foxa2

Our analyses show that in β-cells Insm1 is frequently bound to chromatin together with Neurod1 and Foxa2, two well characterized transcription factors that control mature β-cell function (Naya *et al*, 1997; Lantz *et al*, 2004; Gao *et al*, 2007, 2010; Gu *et al*, 2010; Mastracci *et al*, 2013). Cultured and primary β-cells differ in important parameters like proliferative activity. SJ β-cells resemble but are not identical to islets in their ability to secrete insulin in response to glucose. Furthermore, the cultured cells also respond to exendin-4 and GIP. Because of the ample material provided by cultured cells, we used SJ β-cells as model for ChIP-seq experiments and identified Insm1, Neurod1 and Foxa2 binding sites. A set of the binding sites associated with genes known to control glucose-dependent insulin secretion was re-tested in ChIP-PCR experiments, and all tested sites were occupied also in isolated islets. *cis*-regulatory

modules that assemble many transcription factors are known to control gene expression (Davidson, 2001; Bonn & Furlong, 2008; Ciofani *et al*, 2012). Interestingly, Insm1/Neurod1/Foxa2 binding sites identified in the *Pdx1*, *MafA* and *Hadh* genes were previously shown to possess enhancer activity (Gerrish *et al*, 2000; Lantz *et al*, 2004; Raum *et al*, 2006). Similarly, a large proportion of the identified sequences tested experimentally displayed *cis*-regulatory activity and β-cell lineage selectivity.

We show here that Insm1, Neurod1 and Foxa2 do not only co-occupy chromatin in β-cells, but Insm1 also directly interacts and co-precipitates with Neurod1 and Foxa2 in the absence of DNA binding. Insm1/Neurod1/Foxa2 binding sites represent high affinity sites, as judged from the number of reads in ChIP-seq experiments. Moreover, in cultured hepatocytes that express Foxa2 endogenously, ectopic expression of Insm1 and Neurod1 can synergistically stimulate transcriptional activity in luciferase assays when fragments containing Insm1/Neurod1/Foxa2 binding sites were tested. Remarkably, sites co-occupied by Insm1/Neurod1/Foxa2 predict a large proportion of the Insm1-dependent gene expression in mature β-cells, and the majority of these are located in intergenic and intronic sequences. In contrast, sites that bind Insm1 only correlate poorly with changed gene expression and are frequently enriched in promoters. Our data explain part of the mechanism by which β-cells maintain maturity and are in accordance with previous findings in other cell and tissue types that indicate that combinatorial transcription factor binding can be used to identify functionally important *cis*-regulatory sequences (Davidson, 2001; Bonn & Furlong, 2008; Ciofani *et al*, 2012).

We further show that the combinatorial binding of Insm1/Neurod1/Foxa2 seems to some degree be conserved and functionally important in humans. Such sequences, when mapped to the human genome, were enriched in human sequence variants associated with glycolytic traits. Sites co-occupied by Insm1/Neurod1/Foxa2 represent thus a functionally important sub-class of Insm1 binding sites in the genome. However, the presence of Insm1/Neurod1/Foxa2 sites is found in genes that are positively or negatively de-regulated in *coInsm1* mutant β-cells. A large fraction (46%) but not all Insm1/Neurod1/Foxa2 sites locate to previously mapped putative enhancer sequences of islets (Tennant *et al*, 2013). Remaining sites might correspond to promoters or poised enhancers containing bivalent histone marks that are thought to respond to external stimuli (Creyghton *et al*, 2010). Together, these data indicate that Insm1 acts as a transcriptional regulator and, in a context-dependent manner, as activator or repressor, together with other factors that modify the function of Insm1/Neurod1/Foxa2. Insm1 is known to recruit histone-modifying factors such as Kdm1a, Hdac1/2, Rcor1-3 and other proteins implicated in transcriptional regulation (Hmg20a/b and Gse1) via its SNAG domain (Welcker *et al*, 2013), and our ongoing work indicates that the recruitment of such factors explains many but not all Insm1-dependent functions in the pancreas (Ulrich Köstner and C.B., unpublished data).

Functional deficits and islet immaturity in *coInsm1* mutant islets

The development and maintenance of a mature functional state of β-cells and other cell types depends on the continuous presence of key transcription factors that define cellular identity (Holmberg & Perlmann, 2012). Nevertheless, distinct genes depend on Insm1 during development and in the adult, and furthermore, DNA binding by Insm1 appears to be dynamic. Thus, only a small proportion (4.9%) of Insm1-dependent genes identified in mature β-cells were also deregulated in developing Insm1 mutant pancreata, and among the five known Insm1 binding sites identified previously in developing β-cells, only one located in the *Insm1* promoter was also identified in this study (Gierl *et al*, 2006; Osipovich *et al*, 2014). In addition, this analysis and previous work demonstrate that mutation of transcription factors in mature β-cells is less disruptive than mutation during development. For instance, among the few commonly deregulated genes identified after *Insm1* mutation in developing and mature β-cells, we identified Insulin-1 (*Ins1*) that was downregulated twofold and 13-fold after mutation of *Insm1* in adult and developing β-cells, respectively. The mature gene expression program of β-cells appears therefore to be more stable, possibly due to epigenetic modifications or the existence of more complex and redundant transcription factor networks.

We show here that conditional ablation of *Insm1* in β-cells of mice results in a failure to secrete insulin in response to glucose challenge. Our data indicate that deficits in glucose uptake and metabolism as well as changes in secretagogue response account for this. Thus, *coInsm1* mutant β-cells respond poorly to high glucose and to modulators of glucose-dependent insulin secretion like incretin or pyruvate. The primary deficit is restricted to glucose-dependent insulin secretion and its modulation by secretagogues. Mutant β-cells remain fully capable of insulin secretion after challenge with arginine or global membrane depolarization with exogenous KCl *in vitro*, excluding a general deficit in the basic secretory machinery. Insulin secretion from isolated islets of *coInsm1* mutant mice and immature (P1) islets under various conditions shows remarkable physiological similarities. Furthermore, comparison of differentially expressed genes reveals a large overlap between *coInsm1* mutant islets and immature β-cells. Thus, mutant β-cells resembled β-cells isolated from newborn animals, but we did not detect evidence for a return to a progenitor state marked for instance by *Ngn3* expression. We noted that Insm1/Neurod1/Foxa2 sites with high factor occupancy cluster around genes important for β-cell identity, for instance *Pdx1* and *Ins1*. Further analyses will show whether such clusters correspond to 'super enhancers' that were proposed to dominate the transcriptional control of cell identity (Hnisz *et al*, 2013), and to what extent such 'super enhancers' change during development and maturation in temporal dynamic patterns.

Materials and Methods

Animals and genotyping analysis

The $Insm1^{flox}$ allele was generated using homologous recombination in embryonic stem (ES) cells (Supplementary Fig S1A). The neomycine casette used for selection in ES cells was removed by standard techniques (Rodriguez *et al*, 2000). Control ($Insm1^{flox/+}$;*RIPCreER* or $Insm1^{flox/lacZ}$) and conditional mutant ($Insm1^{flox/lacZ}$;*RIPCreER*) mice were generated by using *RIPCreER* (Dor *et al*, 2004) and $Insm1^{LacZ/+}$ (Gierl *et al*, 2006) strains. Male animals at an age of 8–12 weeks were used. Tamoxifen pellets (25 mg, 21 d release) were inserted under the skin of 4- or 8-week-old mice (control and conditional mutant animals). The *mT/mG* reporter strain was used for verification

of recombination (Muzumdar *et al*, 2007). Phenotypes were analyzed on a mixed C57Bl/6;129Ola background and mutants were always compared with littermates. *RIPCreER* was reported to be expressed also in brain neurons, but Insm1 is solely expressed in neuronal progenitor cells but not neurons, precluding recombination in the nervous system. Genotyping primers are listed in Supplementary Table S9. All breeding, housing and experiments were conducted in accordance with institutional German regulations.

Quantification of insulin levels, glucose levels and β-cells

Blood glucose and blood insulin measurements were performed as described (Poy *et al*, 2009). Average blood glucose levels were determined from average levels of at least six independent measurements of 12–14 individual animals/genotype. For blood insulin levels, average levels were determined from average values obtained from at least two independent measurements of 14–16 individual animals/genotype. Sample sizes chosen were similar as the ones previously reported to provide statistical significance (Kulkarni *et al*, 2002; Kubota *et al*, 2004; Poy *et al*, 2009). For glucose tolerance tests, glucose was injected intraperitoneally (2 g/kg body weight), and blood glucose levels were measured using a glucose meter (Bayer, Leverkusen, Germany). For insulin secretion, glucose (2 g/kg body weight) or arginine (0.3 g/kg body weight) was injected intraperitoneally, and insulin was measured from serum using an ultra sensitive mouse insulin ELISA kit (Crystal Chem. Inc., Downers Grove, USA). Pancreatic insulin content was determined from pancreas tissue extracted with acid ethanol using ELISA (Poy *et al*, 2009). In short, 3 pancreata/genotypes were collected in 5 ml acidic ethanol (2% concentrated HCl in 100% ethanol) and grinded. After centrifugation, supernatants were collected, and insulin concentration was determined by ELISA (Mouse High Range Insulin ELISA, Alpco, USA).

Pancreatic *Ins1* and *Ins2* mRNA was determined by qRT–PCR. The β-cell mass and β-cell number/mm^2 pancreas were determined as described using 3 mice/genotype (Poy *et al*, 2009). In short, every 20^{th} sections (8 μm) of pancreata were collected, that is, 6–8 sections/pancreas encompassing the whole organ, and β-cell area was identified by immunohistology using anti-insulin antibodies. The entire pancreas area, insulin-positive area and pancreas weight before sectioning were determined and used to calculate β-cell mass. The number of β-cells/pancreas area was determined from counts of β-cells ($DAPI^+$ nuclei in $insulin^+$ area) on sections of 90–120 islets/mouse.

Immunohistochemistry, immunoprecipitation and Western blot

Immunohistochemistry was performed as described by Poy *et al* (2009). Fluorescence was imaged on a Zeiss LSM 700 confocal microscope and processed using Adobe Photoshop software. Immunoprecipitation and Western blot were performed as described (Welcker *et al*, 2013). Antibodies used are listed in Supplementary Table S9. For co-immunoprecipitations, SJ β-cells were lysed and centrifuged, and the supernatant was incubated with the indicated antibodies. Antibodies were immobilized on protein A or G beads and used to precipitate endogenous proteins. Beads were washed 3 times with PBS containing 0.02% Tween-20, and protein was eluted using 4% SDS in 0.1 M Tris–HCl pH 7.4.

Isolation of pancreatic islets and analysis of insulin secretion from isolated islets

Pancreatic islets were isolated as described by Poy *et al* (2009). After enrichment on Histopaque (Sigma-Aldrich, Munich, Germany) step gradients, individual islets were picked with a pipette under the microscope.

Insulin secretion from isolated islets (n = 3–4) and SJ β-cells (n = 3) was measured after incubation with the various secretagogues (Poy *et al*, 2004). For this, isolated islets were cultured overnight in RPMI medium (Gibco, Darmstadt, Germany) containing 10% fetal calf serum for recovery. Islets were prepared for analysis by washing in secretion buffer (137 mM NaCl, 0.9 mM $CaCl_2$, 2.7 mM KCl, 1.5 mM KH_2PO_4, 0.5 mM $MgCl_2$, 8.1 mM Na_2HPO_4, 20 mM HEPES pH 7.4, 0.2% BSA), incubation in secretion buffer containing 5.5 mM glucose (30 min) and again washing in secretion buffer. The assay was then performed by incubation for 30 min in secretion buffer containing indicated concentrations of glucose and secretagogues. Released insulin was quantified using ELISA (Mouse High Range Insulin ELISA, Alpco, USA).

Microarray analysis

Total RNA from isolated islets was isolated using TRIzol reagent (Invitrogen, Carlsbad, USA). Genome-wide transcript analysis was performed using Affymetrix GeneChip Mouse Genome 430 2.0 arrays (8 microarrays/genotype, Grossmann *et al*, 2009) according to the manufacturer's protocol. Microarray data were analyzed with R bioconductor package (Huber & Gentleman, 2004) and processed with affy and limma packages. To compare samples, we applied log2 transformation and normalized with the 'quantile' method. Only probes with log2 intensity > 7 were considered for further analysis. The Benjamini–Hochberg FDR method was used to calculate *P*-values (cutoff 0.05). The significance of overlaps in gene expression changes in various models was compared using the hypergeometric probability test http://www.geneprof.org/GeneProf/tools/hypergeometric.jsp.

qRT–PCR analysis

For qRT–PCR analysis, cDNA from five animals/genotype was synthetized using SuperScript III (Invitrogen) and independently analyzed using Absolute qPCR SYBR Green mix (AbGene) on a Bio-Rad C1000 Thermal Cycler (Sheean *et al*, 2014). Expression levels were determined using the $2^{-\Delta\Delta Ct}$ method using *ActB* as internal standard.

ChIP-seq and ChIP-PCR

We generated a new pancreatic β-cell line using a described protocol (Radvanyi *et al*, 1993) in order to obtain cells with low passage number and good physiological response to glucose for ChIP-seq analysis.

Specificities of anti-Insm1 antibody were tested by immunohistochemistry and Western blotting on tissue from control and *Insm1* mutant mice, and of Neurod1 and Foxa2 antibodies by Western blotting (Supplementary Fig S4C). Chromatin precipitation was done essentially as described by Lee *et al* (2006). The PCR primers used

for chromatin analysis are shown in Supplementary Table S9. ChIP-PCR performed with anti-Insm1, anti-Neurod1 and anti-Foxa2 antibodies relied on the use of protein A (Insm1, Neurod1) and protein G (Foxa2) beads. Shown for ChIP-PCR are data from one experiment representative of 2–3 samples (Gao *et al*, 2008).

Chromatin-immunoprecipitated DNA was used to prepare Illumina ChIP-seq (Insm1, Neurod1, Foxa2 and IgG controls) libraries according to the manufacturers' protocol. In brief, starting from 10–20 ng of ChIP-DNA, the following library preparation steps were performed for each sample (Pasquali *et al*, 2014): end-repair, A-tailing, adapter ligation, gel purification and a final PCR enrichment. After quality control on an Agilent Bioanalyzer and quantification of the final library on a Qubit, we proceeded with cluster generation and sequencing. Single-end 51-nt reads were generated, and reads that did not pass the Illumina chastity filter were filtered out. The number of reads obtained from the libraries used to compare Insm1 (148×10^6, 189×10^6), Neurod1 (114×10^6) and Foxa2 (36×10^6, 45×10^6) sites was on average 79% mappable (see also computational analyses). The data were visualized using the UCSC genome browser.

Computational analyses

Reads obtained by sequencing of the libraries were mapped to the mouse (mm9) genome using Bowtie. Reads that mapped with more than 2 mismatches or to more than one position were discarded from further analysis. Peaks were called using Macs software (Zhang *et al*, 2008) with default parameters. To visualize peaks in UCSC genome browser, the Bowtie output was converted to a BigWig format. We assigned a read cutoff to binding sites. For the first Insm1 ChIP-seq experiment, a peak height of 60 was taken as a cutoff. The cutoffs of all further experiments were accordingly normalized to the total number of mapped reads. Two independent ChIP-seq data sets for Insm1 and Foxa2 binding were generated, and we considered only those sites present in both replicates for further analysis (Supplementary Fig S4B). The two replicates of Neurod1 were dissimilar in coverage but displayed large overlap; for the analysis, the single data set with higher coverage was used.

Start and end coordinates of the binding sites were defined as the positions were the number of reads reached 50% of the peak height. Consensus binding site coordinates were then defined as the minimum start and maximum end of the peaks that were defined in the two replicates. Binding sites were annotated as being located in promoter, UTR, intron or exon sequences using the UCSC RefSeq table. When a particular binding site fell into several categories, it was scored only once, according to the following priorities: promoter, UTR, intron and exon. Data processing and visualization was performed with PERL and R scripts. To define the significance in correlation between changes in gene expression and presence of Insm1 or Insm1/Neurod1/Foxa2 binding sites, we used Fisher's exact test.

Motif analysis in identified binding regions was done using MEME (Bailey *et al*, 2009); 500 binding sites containing the highest peak counts were used for analysis. To define in the entire data set numbers of sites containing a motif, we used FIMO (Grant *et al*, 2011) (P-value $< 10^{-3}$). The motif search was applied to ±25 nucleotides around the peak mode. GO term analysis was performed by using the MGI Gene Ontology Term Finder (http://www.informatics.jax.org/gotools/MGI_Term_Finder.html).

The correlation between deregulated genes in coInsm1 mutant islets and various categories of binding sites was analyzed, and the best correlation was found for Insm1/Neurod1/Foxa2 sites. This analysis was complicated by the fact that genes often contain two or more binding sites (e.g., Insm1/Neurod1/Foxa2 and Insm1 only site). Therefore, equivalent analyses were performed after excluding genes with binding sites of multiple categories. Insm1/Neurod1/Foxa2 sites remained the most enriched category in deregulated genes (data summarized in Supplementary Table S5). Insm1 sites were converted to human (hg19) coordinates with UCSC liftOver tool. SNPs with genome-wide association for 14 traits in European individuals were retrieved from the GWAS catalog (P-value $< 5 \times 10^{-8}$) (Hindorff *et al*, 2014). The list of SNPs were pruned using PLINK tools with the following command: –indep-pairwise 100 10 0.2 (Purcell *et al*, 2007), generating a list of index SNPs. The pruning step eliminates SNPs that are in linkage disequilibrium and results in a list of index SNPs in which each disease associated locus is represented by a single SNP. Each index SNP was used to identify sequence variants in high linkage disequilibrium ($r^2 > 0.8$), creating a final SNP list. The variants were identified in the 1,000 Genomes Project CEU (Utah residents of northern and western European ancestry) pilot 1 data. Insm1 binding sites (±250 bp of the start and end of the binding site defined as the positions where the number of reads reached 50% of the peak height) that overlapped with the final SNP list were identified. To test for enrichment, we generated a random set of sequences of identical length with the same genome annotation (such as intron, exon, promoter, UTR) as the Insm1 binding site data set and again tested for the presence SNPs in these sequences. The procedure was repeated 10,000 times. The P-values were calculated as the fraction of runs in which the number of SNPs in random sequences was as large or larger than the number of SNPs in Insm1 binding sites.

Electron microscopy

Pancreata from mice were fixed in 4% formaldehyde in phosphate buffer and postfixed in 2% formaldehyde and 1% glutaraldehyde in phosphate buffer. After treatment with 1% osmium tetroxide and dehydration, the tissue was embedded in Poly/Bed 812 (Polysciences, Inc., Eppelheim, Germany). Ultrathin sections were stained with uranyl acetate and lead citrate and examined using a FEI Morgagni electron microscope. Digital images were taken with a Morada CCD camera and the iTEM software (Olympus Soft Imaging Solutions GmbH, Münster, Germany).

Luciferase assays and siRNA experiments

DNA fragments (average size 678 bp; the exact sequence coordinates are given in Supplemental Table S9) were cloned upstream of a minimal promoter driving the firefly luciferase gene (pGL4.23 [luc2/minP] vector; Promega). The selected fragments were derived from genes whose expression was deregulated in co-Insm1 mutant islets and had been assigned as bound by Insm1 using ChIP-seq in SJ β-cells and ChIP-PCR of isolated islets. Using Lipofectamine 2000 (Invitrogen), SJ β-cells, HepG2 or HEK293 cells were transfected with the firefly luciferase plasmid containing putative *cis*-regulatory

sequences; as an internal control, *Renilla* luciferase plasmid (pRL-TK *Renilla*; Promega) was co-transfected. Cell lysates were prepared 24 h after transfection, and luciferase activity was determined using Dual-Luciferase® Reporter Assay kits (Promega). For each sample ($n = 4$, Ciofani *et al*, 2012), firefly luciferase values were normalized to *Renilla* luciferase values. We display relative luciferase activity as a fold change compared to empty pGL4.23 vector.

siRNAs against *Insm1*, *Neurod1* and *Foxa2* mRNAs were delivered by electroporation using Amaxa kit V and program G-16 according to the protocol provided by the manufacturer. Mouse Insm1 and non-targeting control siRNAs were purchased from Dharmacon (J-049233 -09/-11/-12 for Insm1 and D-001810-10 for control). Mouse Neurod1 and Foxa2 siRNAs were purchased from Ambion (s201725, s67628).

Data availability

Relevant gene expression and ChIP-seq data have been deposited in the GEO database under the following accession numbers: GSE54044 and GSE54046.

Supplementary information for this article is available online: http://emboj.embopress.org

Acknowledgements
We want to thank Michael Strehle (MDC Berlin) for help during computational analyses and preparation of the manuscript, Bettina Brandt for technical assistance, Petra Stallerow and Claudia Päseler for expert animal husbandry support, and Gabriele Born for performing microarray hybridizations (all at the MDC, Berlin). We also thank Malgorzata Borowiak (Baylor College of Medicine, Houston, Texas), Walter Birchmeier, Matthias Treier and Uwe Ohler (MDC, Berlin) for helpful discussions and critical reading of the manuscript. This work was supported by a grant from the BIH to C.B. and a grant of the China Scholarship Council (CSC) to W.S.

Author contributions
SJ performed genetic, biochemical and physiological experiments, experimentally confirmed computational data and designed experiments; AI performed computational analyses. DB generated the Insm1flox strain, WS generated ChIP-seq libraries and sequences, TM helped with generation of confocal images and figures, BP performed electron microscopy, WC, MNP and NR supervised library production/deep sequencing, physiological experiments and computational analysis, respectively. CB supervised the project and wrote the article.

Conflict of interest
The authors declare that they have no conflict of interest.

References

Ahlgren U, Jonsson J, Jonsson L, Simu K, Edlund H (1998) beta-cell-specific inactivation of the mouse Ipf1/Pdx1 gene results in loss of the beta-cell phenotype and maturity onset diabetes. *Genes Dev* 12: 1763 – 1768

Artner I, Hang Y, Mazur M, Yamamoto T, Guo M, Lindner J, Magnuson MA, Stein R (2010) MafA and MafB regulate genes critical to beta-cells in a unique temporal manner. *Diabetes* 59: 2530 – 2539

Babenko AP, Polak M, Cave H, Busiah K, Czernichow P, Scharfmann R, Bryan J, Aguilar-Bryan L, Vaxillaire M, Froguel P (2006) Activating mutations in the ABCC8 gene in neonatal diabetes mellitus. *N Engl J Med* 355: 456 – 466

Baggio LL, Drucker DJ (2007) Biology of incretins: GLP-1 and GIP. *Gastroenterology* 132: 2131 – 2157

Bailey TL, Boden M, Buske FA, Frith M, Grant CE, Clementi L, Ren J, Li WW, Noble WS (2009) MEME SUITE: tools for motif discovery and searching. *Nucleic Acids Res* 37: W202 – W208

Becker TC, BeltrandelRio H, Noel RJ, Johnson JH, Newgard CB (1994) Overexpression of hexokinase I in isolated islets of Langerhans via recombinant adenovirus. Enhancement of glucose metabolism and insulin secretion at basal but not stimulatory glucose levels. *J Biol Chem* 269: 21234 – 21238

Blum B, Hrvatin SS, Schuetz C, Bonal C, Rezania A, Melton DA (2012) Functional beta-cell maturation is marked by an increased glucose threshold and by expression of urocortin 3. *Nat Biotechnol* 30: 261 – 264

Bonn S, Furlong EE (2008) cis-Regulatory networks during development: a view of Drosophila. *Curr Opin Genet Dev* 18: 513 – 520

Breslin MB, Zhu M, Notkins AL, Lan MS (2002) Neuroendocrine differentiation factor, IA-1, is a transcriptional repressor and contains a specific DNA-binding domain: identification of consensus IA-1 binding sequence. *Nucleic Acids Res* 30: 1038 – 1045

Carvalho CP, Barbosa HC, Britan A, Santos-Silva JC, Boschero AC, Meda P, Collares-Buzato CB (2010) Beta cell coupling and connexin expression change during the functional maturation of rat pancreatic islets. *Diabetologia* 53: 1428 – 1437

Ciofani M, Madar A, Galan C, Sellars M, Mace K, Pauli F, Agarwal A, Huang W, Parkurst CN, Muratet M, Newberry KM, Meadows S, Greenfield A, Yang Y, Jain P, Kirigin FK, Birchmeier C, Wagner EF, Murphy KM, Myers RM *et al* (2012) A validated regulatory network for Th17 cell specification. *Cell* 151: 289 – 303

Colsoul B, Schraenen A, Lemaire K, Quintens R, Van Lommel L, Segal A, Owsianik G, Talavera K, Voets T, Margolskee RF, Kokrashvili Z, Gilon P, Nilius B, Schuit FC, Vennekens R (2010) Loss of high-frequency glucose-induced Ca2 + oscillations in pancreatic islets correlates with impaired glucose tolerance in Trpm5-/- mice. *Proc Natl Acad Sci USA* 107: 5208 – 5213

Creyghton MP, Cheng AW, Welstead GG, Kooistra T, Carey BW, Steine EJ, Hanna J, Lodato MA, Frampton GM, Sharp PA, Boyer LA, Young RA, Jaenisch R (2010) Histone H3K27ac separates active from poised enhancers and predicts developmental state. *Proc Natl Acad Sci USA* 107: 21931 – 21936

D'Amour KA, Bang AG, Eliazer S, Kelly OG, Agulnick AD, Smart NG, Moorman MA, Kroon E, Carpenter MK, Baetge EE (2006) Production of pancreatic hormone-expressing endocrine cells from human embryonic stem cells. *Nat Biotechnol* 24: 1392 – 1401

Davidson EH (2001) *Genomic Regulatory Systems: Development and Evolution*. San Diego: Academic Press Inc.

Dor Y, Brown J, Martinez OI, Melton DA (2004) Adult pancreatic beta-cells are formed by self-duplication rather than stem-cell differentiation. *Nature* 429: 41 – 46

Dor Y, Glaser B (2013) beta-cell dedifferentiation and type 2 diabetes. *N Engl J Med* 368: 572 – 573

Gao N, White P, Doliba N, Golson ML, Matschinsky FM, Kaestner KH (2007) Foxa2 controls vesicle docking and insulin secretion in mature Beta cells. *Cell Metab* 6: 267 – 279

Gao N, LeLay J, Vatamaniuk MZ, Rieck S, Friedman JR, Kaestner KH (2008) Dynamic regulation of Pdx1 enhancers by Foxa1 and Foxa2 is essential for pancreas development. *Genes Dev* 22: 3435 – 3448

Gao N, Le Lay J, Qin W, Doliba N, Schug J, Fox AJ, Smirnova O, Matschinsky FM, Kaestner KH (2010) Foxa1 and Foxa2 maintain the metabolic

and secretory features of the mature beta-cell. *Mol Endocrinol* 24: 1594 – 1604

Gerrish K, Gannon M, Shih D, Henderson E, Stoffel M, Wright CV, Stein R (2000) Pancreatic beta cell-specific transcription of the pdx-1 gene. The role of conserved upstream control regions and their hepatic nuclear factor 3beta sites. *J Biol Chem* 275: 3485 – 3492

Gierl MS, Karoulias N, Wende H, Strehle M, Birchmeier C (2006) The zinc-finger factor Insm1 (IA-1) is essential for the development of pancreatic beta cells and intestinal endocrine cells. *Genes Dev* 20: 2465 – 2478

Grant CE, Bailey TL, Noble WS (2011) FIMO: scanning for occurrences of a given motif. *Bioinformatics* 27: 1017 – 1018

Grossmann KS, Wende H, Paul FE, Cheret C, Garratt AN, Zurborg S, Feinberg K, Besser D, Schulz H, Peles E, Selbach M, Birchmeier W, Birchmeier C (2009) The tyrosine phosphatase Shp2 (PTPN11) directs Neuregulin-1/ErbB signaling throughout Schwann cell development. *Proc Natl Acad Sci USA* 106: 16704 – 16709

Gu C, Stein GH, Pan N, Goebbels S, Hornberg H, Nave KA, Herrera P, White P, Kaestner KH, Sussel L, Lee JE (2010) Pancreatic beta cells require NeuroD to achieve and maintain functional maturity. *Cell Metab* 11: 298 – 310

Guillam MT, Hummler E, Schaerer E, Yeh JI, Birnbaum MJ, Beermann F, Schmidt A, Deriaz N, Thorens B (1997) Early diabetes and abnormal postnatal pancreatic islet development in mice lacking Glut-2. *Nat Genet* 17: 327 – 330

Halban PA, Wollheim CB, Blondel B, Meda P, Niesor EN, Mintz DH (1982) The possible importance of contact between pancreatic islet cells for the control of insulin release. *Endocrinology* 111: 86 – 94

Hang Y, Yamamoto T, Benninger RK, Brissova M, Guo M, Bush W, Piston DW, Powers AC, Magnuson M, Thurmond DC, Stein R (2014) The MafA transcription factor becomes essential to islet beta-cells soon after birth. *Diabetes* 63: 1994 – 2005

Hindorff LA, MacArthur JEBI, Morales JEBI, Junkins HA, Hall PN, Klemm AK, Manolio TA (2014) A Catalog of Published Genome-Wide Association Studies. Available at: www.genome.gov/gwastudies

Hnisz D, Abraham BJ, Lee TI, Lau A, Saint-Andre V, Sigova AA, Hoke HA, Young RA (2013) Super-enhancers in the control of cell identity and disease. *Cell* 155: 934 – 947

Holland AM, Hale MA, Kagami H, Hammer RE, MacDonald RJ (2002) Experimental control of pancreatic development and maintenance. *Proc Natl Acad Sci USA* 99: 12236 – 12241

Holmberg J, Perlmann T (2012) Maintaining differentiated cellular identity. *Nat Rev Genet* 13: 429 – 439

Huber W, Gentleman R (2004) matchprobes: a Bioconductor package for the sequence-matching of microarray probe elements. *Bioinformatics* 20: 1651 – 1652

Kluth O, Matzke D, Schulze G, Schwenk RW, Joost HG, Schurmann A (2014) Differential transcriptome analysis of diabetes-resistant and -sensitive mouse islets reveals significant overlap with human diabetes susceptibility genes. *Diabetes* 63: 4230 – 4238

Kubota N, Terauchi Y, Tobe K, Yano W, Suzuki R, Ueki K, Takamoto I, Satoh H, Maki T, Kubota T, Moroi M, Okada-Iwabu M, Ezaki O, Nagai R, Ueta Y, Kadowaki T, Noda T (2004) Insulin receptor substrate 2 plays a crucial role in beta cells and the hypothalamus. *J Clin Invest* 114: 917 – 927

Kulkarni RN, Holzenberger M, Shih DQ, Ozcan U, Stoffel M, Magnuson MA, Kahn CR (2002) beta-cell-specific deletion of the Igf1 receptor leads to hyperinsulinemia and glucose intolerance but does not alter beta-cell mass. *Nat Genet* 31: 111 – 115

Lai JS, Herr W (1992) Ethidium bromide provides a simple tool for identifying genuine DNA-independent protein associations. *Proc Natl Acad Sci USA* 89: 6958 – 6962

Lang J (1999) Molecular mechanisms and regulation of insulin exocytosis as a paradigm of endocrine secretion. *Eur J Biochem* 259: 3 – 17

Lantz KA, Vatamaniuk MZ, Brestelli JE, Friedman JR, Matschinsky FM, Kaestner KH (2004) Foxa2 regulates multiple pathways of insulin secretion. *J Clin Invest* 114: 512 – 520

Lee TI, Johnstone SE, Young RA (2006) Chromatin immunoprecipitation and microarray-based analysis of protein location. *Nat Protoc* 1: 729 – 748

Leroux L, Desbois P, Lamotte L, Duvillie B, Cordonnier N, Jackerott M, Jami J, Bucchini D, Joshi RL (2001) Compensatory responses in mice carrying a null mutation for Ins1 or Ins2. *Diabetes* 50(Suppl 1): S150 – S153

MacDonald PE, Joseph JW, Rorsman P (2005) Glucose-sensing mechanisms in pancreatic beta-cells. *Philos Trans R Soc Lond B Biol Sci* 360: 2211 – 2225

Mastracci TL, Anderson KR, Papizan JB, Sussel L (2013) Regulation of Neurod1 contributes to the lineage potential of Neurogenin3 + endocrine precursor cells in the pancreas. *PLoS Genet* 9: e1003278

Mellitzer G, Bonne S, Luco RF, Van De Casteele M, Lenne-Samuel N, Collombat P, Mansouri A, Lee J, Lan M, Pipeleers D, Nielsen FC, Ferrer J, Gradwohl G, Heimberg H (2006) IA1 is NGN3-dependent and essential for differentiation of the endocrine pancreas. *EMBO J* 25: 1344 – 1352

van der Meulen T, Xie R, Kelly OG, Vale WW, Sander M, Huising MO (2012) Urocortin 3 marks mature human primary and embryonic stem cell-derived pancreatic alpha and beta cells. *PLoS ONE* 7: e52181

Morris AP, Voight BF, Teslovich TM, Ferreira T, Segre AV, Steinthorsdottir V, Strawbridge RJ, Khan H, Grallert H, Mahajan A, Prokopenko I, Kang HM, Dina C, Esko T, Fraser RM, Kanoni S, Kumar A, Lagou V, Langenberg C, Luan J *et al* (2012) Large-scale association analysis provides insights into the genetic architecture and pathophysiology of type 2 diabetes. *Nat Genet* 44: 981 – 990

Muzumdar MD, Tasic B, Miyamichi K, Li L, Luo L (2007) A global double-fluorescent Cre reporter mouse. *Genesis* 45: 593 – 605

Naya FJ, Huang HP, Qiu Y, Mutoh H, DeMayo FJ, Leiter AB, Tsai MJ (1997) Diabetes, defective pancreatic morphogenesis, and abnormal enteroendocrine differentiation in BETA2/neuroD-deficient mice. *Genes Dev* 11: 2323 – 2334

Newburger DE, Bulyk ML (2009) UniPROBE: an online database of protein binding microarray data on protein-DNA interactions. *Nucleic Acids Res* 37: D77 – D82

Nostro MC, Keller G (2012) Generation of beta cells from human pluripotent stem cells: potential for regenerative medicine. *Semin Cell Dev Biol* 23: 701 – 710

Osipovich AB, Long Q, Manduchi E, Gangula R, Hipkens SB, Schneider J, Okubo T, Stoeckert CJ Jr, Takada S, Magnuson MA (2014) Insm1 promotes endocrine cell differentiation by modulating the expression of a network of genes that includes Neurog3 and Ripply3. *Development* 141: 2939 – 2949

Pagliuca FW, Millman JR, Gurtler M, Segel M, Van Dervort A, Ryu JH, Peterson QP, Greiner D, Melton DA (2014) Generation of functional human pancreatic beta cells in vitro. *Cell* 159: 428 – 439

Pasquali L, Gaulton KJ, Rodriguez-Segui SA, Mularoni L, Miguel-Escalada I, Akerman I, Tena JJ, Moran I, Gomez-Marin C, van de Bunt M, Ponsa-Cobas J, Castro N, Nammo T, Cebola I, Garcia-Hurtado J, Maestro MA, Pattou F, Piemonti L, Berney T, Gloyn AL *et al* (2014) Pancreatic islet enhancer clusters enriched in type 2 diabetes risk-associated variants. *Nat Genet* 46: 136 – 143

Poy MN, Eliasson L, Krutzfeldt J, Kuwajima S, Ma X, Macdonald PE, Pfeffer S, Tuschl T, Rajewsky N, Rorsman P, Stoffel M (2004) A pancreatic islet-specific microRNA regulates insulin secretion. *Nature* 432: 226 – 230

Poy MN, Hausser J, Trajkovski M, Braun M, Collins S, Rorsman P, Zavolan M, Stoffel M (2009) miR-375 maintains normal pancreatic alpha- and beta-cell mass. *Proc Natl Acad Sci USA* 106: 5813 – 5818

Purcell S, Neale B, Todd-Brown K, Thomas L, Ferreira MA, Bender D, Maller J, Sklar P, de Bakker PI, Daly MJ, Sham PC (2007) PLINK: a tool set for whole-genome association and population-based linkage analyses. *Am J Hum Genet* 81: 559 – 575

Radvanyi F, Christgau S, Baekkeskov S, Jolicoeur C, Hanahan D (1993) Pancreatic beta cells cultured from individual preneoplastic foci in a multistage tumorigenesis pathway: a potentially general technique for isolating physiologically representative cell lines. *Mol Cell Biol* 13: 4223 – 4232

Raum JC, Gerrish K, Artner I, Henderson E, Guo M, Sussel L, Schisler JC, Newgard CB, Stein R (2006) FoxA2, Nkx2.2, and PDX-1 regulate islet beta-cell-specific mafA expression through conserved sequences located between base pairs -8,118 and -7,750 upstream from the transcription start site. *Mol Cell Biol* 26: 5735 – 5743

Rodriguez CI, Buchholz F, Galloway J, Sequerra R, Kasper J, Ayala R, Stewart AF, Dymecki SM (2000) High-efficiency deleter mice show that FLPe is an alternative to Cre-loxP. *Nat Genet* 25: 139 – 140

Rorsman P, Arkhammar P, Bokvist K, Hellerstrom C, Nilsson T, Welsh M, Welsh N, Berggren PO (1989) Failure of glucose to elicit a normal secretory response in fetal pancreatic beta cells results from glucose insensitivity of the ATP-regulated K+ channels. *Proc Natl Acad Sci USA* 86: 4505 – 4509

Scott RA, Lagou V, Welch RP, Wheeler E, Montasser ME, Luan J, Magi R, Strawbridge RJ, Rehnberg E, Gustafsson S, Kanoni S, Rasmussen-Torvik LJ, Yengo L, Lecoeur C, Shungin D, Sanna S, Sidore C, Johnson PC, Jukema JW, Johnson T *et al* (2012) Large-scale association analyses identify new loci influencing glycemic traits and provide insight into the underlying biological pathways. *Nat Genet* 44: 991 – 1005

Sheean ME, McShane E, Cheret C, Walcher J, Muller T, Wulf-Goldenberg A, Hoelper S, Garratt AN, Kruger M, Rajewsky K, Meijer D, Birchmeier W, Lewin GR, Selbach M, Birchmeier C (2014) Activation of MAPK overrides the termination of myelin growth and replaces Nrg1/ErbB3 signals during Schwann cell development and myelination. *Genes Dev* 28: 290 – 303

Stanojevic V, Habener JF, Holz GG, Leech CA (2008) Cytosolic adenylate kinases regulate K-ATP channel activity in human beta-cells. *Biochem Biophys Res Commun* 368: 614 – 619

Sugden MC, Holness MJ (2013) The pyruvate carboxylase-pyruvate dehydrogenase axis in islet pyruvate metabolism: going round in circles? *Islets* 3: 302 – 319

Szabat M, Lynn FC, Hoffman BG, Kieffer TJ, Allan DW, Johnson JD (2012) Maintenance of beta-cell maturity and plasticity in the adult pancreas: developmental biology concepts in adult physiology. *Diabetes* 61: 1365 – 1371

Taylor BL, Liu FF, Sander M (2013) Nkx6.1 is essential for maintaining the functional state of pancreatic beta cells. *Cell Rep* 4: 1262 – 1275

Tennant BR, Robertson AG, Kramer M, Li L, Zhang X, Beach M, Thiessen N, Chiu R, Mungall K, Whiting CJ, Sabatini PV, Kim A, Gottardo R, Marra MA, Lynn FC, Jones SJ, Hoodless PA, Hoffman BG (2013) Identification and analysis of murine pancreatic islet enhancers. *Diabetologia* 56: 542 – 552

Truax AD, Greer SF (2012) ChIP and Re-ChIP assays: investigating interactions between regulatory proteins, histone modifications, and the DNA sequences to which they bind. *Methods Mol Biol* 809: 175 – 188

Tseng CC, Zhang XY (1998) Role of regulator of G protein signaling in desensitization of the glucose-dependent insulinotropic peptide receptor. *Endocrinology* 139: 4470 – 4475

Wang Y, Martin CC, Oeser JK, Sarkar S, McGuinness OP, Hutton JC, O'Brien RM (2007) Deletion of the gene encoding the islet-specific glucose-6-phosphatase catalytic subunit-related protein autoantigen results in a mild metabolic phenotype. *Diabetologia* 50: 774 – 778

Wang Z, York NW, Nichols CG, Remedi MS (2014) Pancreatic beta Cell Dedifferentiation in Diabetes and Redifferentiation following Insulin Therapy. *Cell Metab* 19: 872 – 882

Weir GC, Bonner-Weir S (2004) Five stages of evolving beta-cell dysfunction during progression to diabetes. *Diabetes* 53(Suppl 3): S16 – S21

Welcker JE, Hernandez-Miranda LR, Paul FE, Jia S, Ivanov A, Selbach M, Birchmeier C (2013) Insm1 controls development of pituitary endocrine cells and requires a SNAG domain for function and for recruitment of histone-modifying factors. *Development* 140: 4947 – 4958

Wildner H, Gierl MS, Strehle M, Pla P, Birchmeier C (2008) Insm1 (IA-1) is a crucial component of the transcriptional network that controls differentiation of the sympatho-adrenal lineage. *Development* 135: 473 – 481

Xu J, Han J, Long YS, Epstein PN, Liu YQ (2008) The role of pyruvate carboxylase in insulin secretion and proliferation in rat pancreatic beta cells. *Diabetologia* 51: 2022 – 2030

Zhang Y, Liu T, Meyer CA, Eeckhoute J, Johnson DS, Bernstein BE, Nusbaum C, Myers RM, Brown M, Li W, Liu XS (2008) Model-based analysis of ChIP-Seq (MACS). *Genome Biol* 9: R137

Ziv O, Glaser B, Dor Y (2013) The plastic pancreas. *Dev Cell* 26: 3 – 7

Published online: March 31, 2015